REVIEW ARTICLE

Simple transport properties of simple metals: classical theories and modern experiments

To cite this article: R J M van Vucht *et al* 1985 *Rep. Prog. Phys.* **48** 853

View the article online for updates and enhancements.

Related content

Recent citations

Simple transport properties of simple metals: classical theories and modern experiments

R J M van Vucht†, H van Kempen and P Wyder‡

Research Institute for Materials, University of Nijmegen, Toernooiveld, 6525 ED Nijmegen, The Netherlands

Abstract

The low-temperature DC electrical and thermal resistance of nearly-free-electron metals, such as the alkali metals and aluminium, are ideal for testing our understanding of the basic scattering processes of electrons and phonons in a metallic environment. The greatly improved experimental capabilities of the past decade facilitated measurements, the results of which made clear that the traditional models were at least incomplete. Significant progress has hence been made in understanding the role of electron–electron and electron–phonon scattering, both normal and Umklapp; their sample dependence; other deviations from Matthiessen's rule; the influence of the lattice thermal conductivity on the transport tensor elements; the linear magnetoresistivity, and related fields. Yet, crucial questions like the existence of a charge density wave ground state in the alkali metals remain open, and new ones show up.

This article was received in August 1984.

† Present address: Philips Medical Systems Division, Building QJ-k, PO Box 218, 5600 MD Eindhoven, The Netherlands.
‡ Present address: Max-Planck-Institut für Festkorperforschung, Hochfeld-Magnetlabor, 166X, F-38042, Grenoble-Cedex, France.

Contents

1. Introduction

1.1. General

The field of transport properties of metals was not widely opened to both experimental and theoretical investigation until the advent of Drude's theory on electronic conduction at the beginning of the century. A real breakthrough, however, occurred when modern quantum theory was applied to periodic structures by Bloch in the 1930s. From that time on, a continuous interaction between theory and experiment, culminating in Ziman's book *Electrons and Phonons* (1960), gave the impression that the transport properties of simple metals were at least in a formal sense well understood. In the late 1960s and the 1970s, when new techniques permitted experimental penetration into the regions of very low temperatures, high magnetic fields, high purities and, in some cases, sub-PPM precision, extrapolations of the established theories often proved inappropriate. This review article is intended to give an account of the recent advances in experiment and theory.

The main topics to be presented are: the appearance and magnitude of an electron-electron scattering term in low-temperature conductivity (§ 2); Umklapp scattering contributions to both the electron–electron and electron–phonon scattering terms; the manifestation of phonon drag in the low-temperature resistivity of the alkali metals; sample dependence of these terms and other deviations from Matthiessen's rule; the influence of the lattice thermal conductivity on the thermal transport tensor elements (§ 3); the linear magnetoresistance (§ 4); and the probability and possible effects of a charge density wave ground state in the alkali metals (§ 5).

First, however, a brief explanation of what we consider simple metals and simple transport properties is required.

1.2. Simple metals and simple transport properties

Our definition of 'simple metals' comprises those metals which can be described by a nearly-free-electron model. Such a model allows basic properties of these metals to be calculated in a simple way because the influence of the lattice can be treated as a small perturbation for the electron gas. Therefore, implications of new theories can be tested most readily by their application to simple metals. The most ubiquitously studied examples are potassium and aluminium, and these metals will be most referred to in this review. The first metal has a nearly spherical Fermi surface, which again simplifies many calculations since the electron properties are expected to be, in many respects, isotropic. Aluminium is the chief example of a polyvalent metal in which the Fermi surface crosses the Brillouin zone boundaries (figure 1). The noble metals gold, silver and copper also possess such multiply connected Fermi surfaces, and will appear frequently in this review in relation to aluminium and its look-alike, indium. However, in a magnetic field the noble metals can no longer be considered simple because their Fermi surface gives rise to open orbits, contrary to aluminium.

The Fermi surfaces of the alkali metals and aluminium have been measured extensively, mainly by the de Haas–van Alphen method (Lee (1971) for the alkali
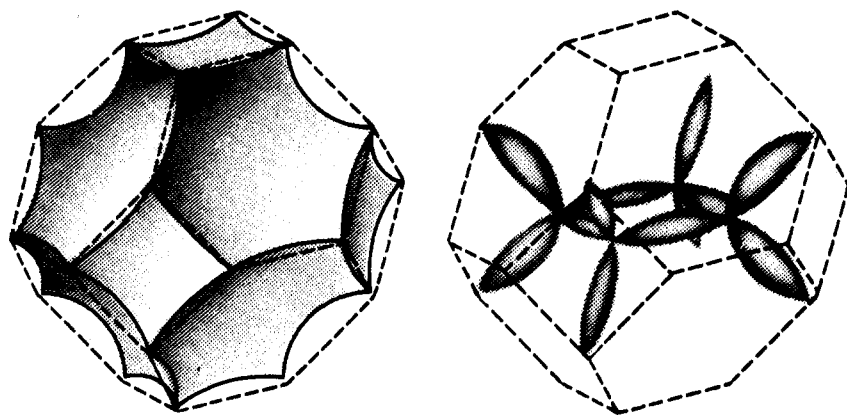
Figure 1. The free-electron Fermi surface of aluminium in the second and third Brillouin zones (from Ashcroft and Mermin 1976). In reality the Fermi surface portions which intersect the Brillouin zone boundaries broaden to form 'necks' in the second zone.

metals; Templeton (1981) for K; Ashcroft (1963) gives references for Al). The alkali metals always exhibit an essentially spherical Fermi surface to within a few per cent, with maximum deviations from sphericity ranging from 0.14% in K to 3.5–5.5% in Li (Lee 1971), where the Fermi surface comes closest to the Brillouin zone boundaries. Usually, there is no significant discrepancy between calculated (Lee 1969, Dagens and Perrot 1973, Perdew and Vosko 1974) and measured Fermi surface properties. An exception is formed by theories that predict a different symmetry: Overhauser (1978) finds that potassium should exhibit a charge density wave ground state, which has far-reaching consequences. In § 5 a short review of the situation regarding this theory is given. A band structure calculation by O'Keefe and Goddard (1969) for lithium resulted in a simple cubic structure with two atoms per unit cell. Such a structure also causes a multiply connected Fermi surface and its consequences are therefore largely similar to that of a charge density wave state, apart from the cubic symmetry which is conserved in this case. This calculation has found no firm experimental evidence, however.

The Fermi surface of aluminium (figure 1) consists of a hole surface in the second zone and a framework of interconnected 'cigars' in the third zone. The second zone surface consists of weakly curved parts far from the Brillouin zone boundaries, and strongly curved regions where the surface intersects these at the 'necks'. The weakly and strongly curved regions can possess largely different properties with regard to scattering lifetimes.

In the following, we confine ourselves to 'simple' transport properties. We look only at the steady-state properties of non-superconducting pure metals and dilute alloys far below the Debye temperature, which ranges from 100 K in potassium to about 430 K in aluminium. This means that only a few phonon states are excited.

In the following three sections we are primarily concerned with electron- and phonon-scattering mechanisms. The two kinds of DC transport of prime interest for studying these mechanisms are electronic conduction, for which electrons are completely responsible, and heat conduction, by both electrons and phonons. The thermopower gives additional information in the form of energy dependence of the scattering. However, in this review, we shall concentrate on the electrical and thermal resistivity.

1.3. Factors influencing the transport properties

For evaluating the transport tensor coefficients of metals, the most successful tool for several decades has been the Boltzmann transport equation (BTE) or kinetic equation (see, for example, Ziman 1972 chap 7, Abrikosov 1972 chap 3). It is easier to obtain results from the BTE in practical cases than from, for example, the mathematically more exact Kubo formalism, and when both methods can be compared in a specific situation, the results are essentially equal. Apart from this method, still other formalisms are being developed for gaining insight in specific fields of transport, among which the diffusion equation method (reviewed by Gurzhi and Kopeliovich (1981)) is quite powerful.

The BTE describes the evolution in time of the electron (or quasi-particle) density in phase space $f(r, k)$, which counts the number of particles in the neighbourhood of a point r in real space and having a momentum k. This restricts its use to the description of wave packets which are not localised completely in either real or momentum space, since they would be completely unlocalised in the other space. At any time, one can compute the electric current density from $f(r, k)$ by

$$ J = J_0 e \int d^3r \int d^3k\, f(r, k) v(k) $$

and the other transport quantities in similar ways.

The BTE is essentially a continuity equation for $f(r, k)$ in which terms are present that account for external forces on the system, and for scattering processes. The latter have the form $\partial f/\partial t|_{\text{coll}}$. In the relaxation time approximation, these are replaced by terms $(f - f_0)/\tau_i$ where f_0 is the phase-space distribution in the absence of external fields and τ_i is the characteristic scattering time for the ith scattering process. In the simplest theory, scattering terms τ_i^{-1} from different scattering processes are assumed to be additive. In that case, if all τ_i are also independent of k, the electron distribution in momentum space is uniformly translated on the application of an electric field, and the simplest approximations leading to Matthiessen's rule (§ 2) are valid. Thus, the transport properties are mainly determined by $f_0(r, k)$ and τ_i. Among the facts that make the picture more involved are the following.

(i) τ generally depends on k, thus changing the actual distribution function f. This affects, in turn, the chance for the particles to be scattered by another anisotropic process. This appears to be the main interference mechanism between scattering mechanisms, more important than interference in the scattering probabilities themselves. We shall show in § 2 that many of the recent developments in the field of electronic transport are related to this effect.

(ii) τ may be energy-dependent: it varies not only parallel to, but also perpendicular to, the Fermi surface. This effect is primarily important for the diffusion thermopower.

(iii) The local shape of the Fermi surface strongly affects $v(k)$ and Umklapp probabilities, thus influencing the effect which scattering processes have on the electrical or thermal current; this makes the polyvalent metals behave differently from the alkali metals. The Fermi surface deformation caused by a charge density wave (see § 5) would also imply drastic changes in the behaviour of alkali metals.

(iv) Magnetic fields also move the electrons over the Fermi surface, changing $f_0(k)$. Their effect can, at least at low fields, be compared to the isotropisation caused by a large impurity density.

(v) At high magnetic fields, the occurrence of Landau quantisation, and eventually of magnetic breakdown, alters the Fermi surface shape and hence $f_0(\mathbf{k})$ significantly.

(vi) Since many scattering times are temperature-dependent, the competition between the various scattering mechanisms may lead to quite different situations in different temperature regions.

In § 2, we shall demonstrate how the electrical resistivity is a major tool for the investigation of these effects. The thermal resistivity gives extra information, primarily by the way in which the Lorentz number is influenced by various scatterers (§ 3). The high-field transport properties, of which the linear magnetoresistance is the most prominent problem (§ 4), were originally thought to arise from the same sort of effects, but recent developments show that extrinsic effects are completely dominating. Other information on scattering processes and Fermi surface effects is obtained by means of the lattice thermal conductivity (§ 3) and methods which fall beyond the scope of this review. Of these, we mention the novel technique of point contact spectroscopy (reviewed by Jansen *et al* (1980)) and ultrasound techniques which give information on electron–phonon coupling, transverse electron focusing (e.g. Tsoi *et al* 1979) which gives information on electron–surface scattering, and the de Haas–van Alphen and Shubnikov–de Haas effects. The latter effects provide insight into the Fermi surface details, and into scattering mechanisms which influence the Dingle temperatures.

2. The low-temperature electrical resistivity

2.1. Introduction

The most commonly measured transport property at low temperatures is the electrical resistivity. Two contributions to it have been known for a long time: a constant term—the residual resistivity ρ_0—caused by electron–impurity and electron–lattice imperfection scattering, and an electron–phonon term which according to the simplest theories should behave in the low-temperature limit approximately as T^5: the ideal resistivity (see, for example, Ziman 1960). Besides these, theorists have long been postulating the existence of a term due to electron–electron scattering which went like T^2 (Landau and Pomeranchuk 1936). Since the residual resistivity is much larger than the other terms at low temperatures, even for the purest and best annealed samples, it was very hard to study the temperature-dependent terms until some 15 years ago. At that time, very high precision techniques were developed which permit us now to measure $\rho(T)$ with a precision of 0.1 PPM at temperatures which are known to within 0.5 mK. This has proved precise enough to discover the electron–electron term (§ 2.4) and to study unexpected phenomena in the electron–phonon term.

As early as 1864, Matthiessen and Vogt measured the T-dependent electrical resistivity at higher temperatures as a function of impurity content. From these measurements, they concluded that to a close approximation the resistivity of an impure metal consists of a temperature-dependent term independent of impurity content, and a constant term which represents the effect of the impurities:

$$\rho(n_i, T) = \rho_0(n_i) + \rho(T).$$

In this formula, lattice defects have an effect similar to impurities.

It turns out that this statement does not hold in most systems. Much theoretical and experimental attention is still concentrated on studying deviations from Mat-

thiessen's rule (DMR). A quite comprehensive review of the situation in this field was given by Bass (1972).

In order to give a feeling of where the modern problems are, we show figures 2 and 3 which demonstrate several aspects of the present situation. In figure 2, the resistivity of potassium at very low temperatures as measured by van Kempen *et al* (1981) is plotted in such a way that an exponential behaviour above 2 K is evident. We ascribe this deviation from the Bloch T^5 term to phonon drag. Below 2 K, another term dominates $\rho(T)$: we identify it with the electron–electron scattering term. The graph demonstrates that the exponential term is nearly sample-independent, but the magnitude of the electron–electron term varies considerably, in these annealed samples monotonically with the residual resistivity.
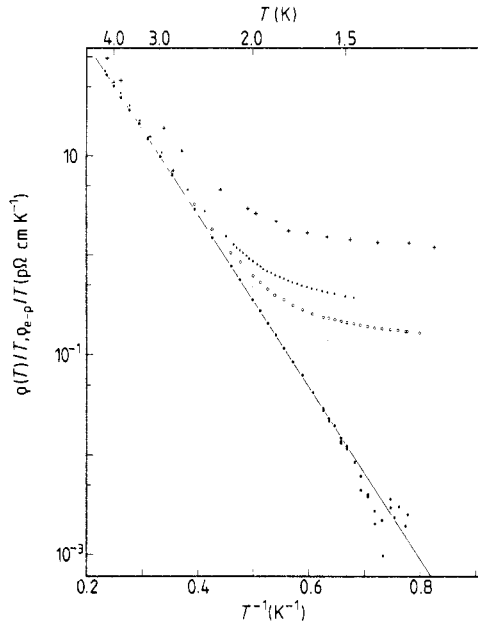
Figure 2. $\rho(T)/T$ of several samples of van Kempen *et al* (1976, 1981) plotted logarithmically as a function of $1/T$ to show the exponential temperature dependence of the temperature-dependent part of the resistivity above 2.5 K. Closed triangles: sample 1 (RRR = 3100); open circles: sample 2b (RRR = 6300); open triangles: sample 2c (RRR = 8100); +: sample 3a (RRR = 390). The closed circles represent the resistivity of sample 2b after subtraction of a T^2 term whose magnitude is determined at the lowest temperatures. An exponential behaviour of $\rho_{e-p}(T)$ down to 1.3 K is consistent with the data.

Figure 3 shows quite the contrary: it contains measurements from Ribot *et al* (1981) on aluminium samples of different purities. The way of plotting is different from the potassium figure in order to demonstrate that, in this case, the temperature behaviour follows closely a $T^2 + T^n$ behaviour, where $n \simeq 5$ at the lowest temperatures. From the purest samples deviations from $n \simeq 5$ start at considerably lower temperatures than for the least pure samples. The magnitude of the electron–electron term (intersection of curves through the data with the vertical axis) is almost sample-independent, but the magnitude and the shape of the electron–phonon term in the purest samples deviate considerably from what we would expect to find from the simplest models.

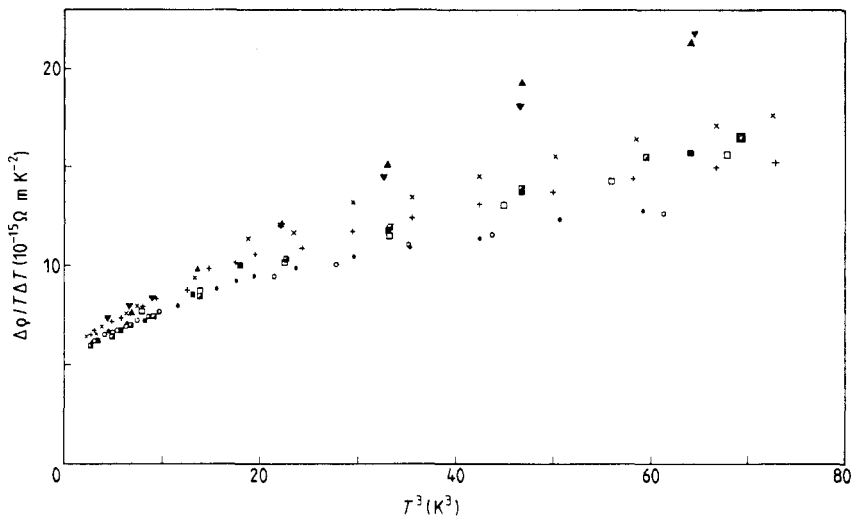**Figure 3.** $\Delta\rho/T\Delta T$ as a function of T^3 for aluminium samples (Ribot *et al* 1981). The value at $T = 0$ represents the magnitude of the electron–electron term. The electron–phonon term is seen to behave like T^5 only over a limited temperature range for impure samples (full triangles: samples 5 (RRR = 255) and 6 (RRR = 245)) and over a much smaller region for pure ones (e.g. full circles: sample 2 with RRR = 40 600).

The following subsections will give a more detailed account of the experimental and theoretical developments from which more insight into these puzzling differences have been obtained.

2.2. High precision resistivity measurements

As an interlude, we describe briefly the technical improvements in the field of electrical resistivity measurements. At low temperatures the sample resistances are usually of the order of a few $\mu\Omega$, so that at maximum currents of 1 A a sensitivity of nanovolts is required to obtain a precision of 0.1%. Nanovoltmeters are commercially available now, making very precise measurements of, for example, magnetoresistance feasible with a classical four-terminal method. A similar precision is attained by several probeless techniques: induced torque, helicons (both described by Delaney (1974)) and eddy current methods (Daybell 1967).

For the exploration of the temperature-dependent resistivity terms below 4 K, a much higher precision of 1 PPM or better is necessary. Figure 4 shows a typical modern system which is in use in Nijmegen (van Kempen *et al* 1979). This system measures the ratio of the sample resistance and the resistance of a reference resistor. These two components are connected in a superconducting circuit together with a superconducting galvanometer, a classical one or a SQUID, which measures the current in the circuit. The reference resistor has a small well-known temperature dependence. In comparable systems, its influence can be entirely eliminated by modulating the sample temperature (Edmunds *et al* 1980) and the temperature derivative of $\rho(T)$ is obtained. Currents of the order of 1 A are delivered to the resistors by very stable externally regulated current sources. The ratio of these currents is adjusted (in the case of figure 4 semi-automatically) until the galvanometer measures zero voltage difference. Then the current ratio can be read by means of a current comparator with a 0.1 PPM precision.
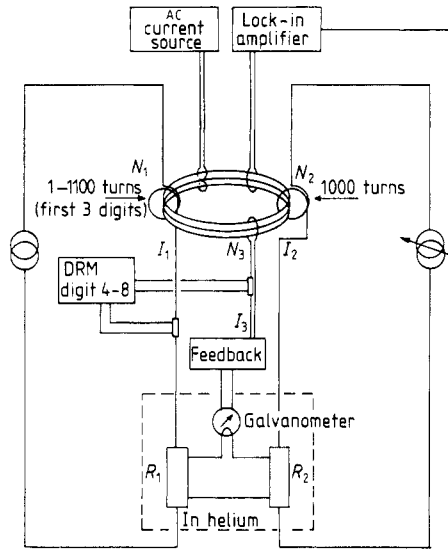
Figure 4. Schematic of the resistance measurement system of the Nijmegen group. A current comparator (top) with a precision of 0.1 PPM supplies two currents I_1 and I_2 to the sample R_1 and the reference resistor R_2. The ratio of these resistances is determined from the ratio of the currents when the superconducting galvanometer measures a zero voltage difference across the resistances. A feedback loop coupled to the galvanometer permits semi-automatic operation. This is used for finding the fourth to eighth digit of the ratio.

The sensitivity of a classical superconducting galvanometer is about 10^{-7} A. SQUID generally offer higher speed and sensitivity, but require more precautions to prevent overloading. The noise level is so low that usually the Johnson noise of the sample and reference resistor limits the obtainable sensitivity.

For a precise determination of the temperature dependence, the temperature itself must also be known to high precision. An extensive discussion of the precautions to be taken can be found in Ribot *et al* (1981).

2.3. Electron-phonon scattering

2.3.1. Normal and Umklapp scattering. The classical Bloch theory for ρ_{e-p} (see Ziman 1960 chap 9.5) is based on the following assumptions.

(i) Only normal scattering processes are allowed (see figure 5) so $k - k' = q_{ph}$.

(ii) The Fermi surface is spherical and τ_{e-p} is independent of k.

(iii) The Debye approximation for the phonon dispersion relation is adopted; only scattering by longitudinal phonons is considered.

(iv) $|v(k)|$ is constant on the Fermi surface.

(v) The phonons stay in thermal equilibrium.

By a variational treatment, one arrives at

$$\rho_{e-p}(T) \propto (T/\theta)^5 \int_0^{\theta/T} \frac{z^5\, dz}{(e^z - 1)(1 - e^{-z})}$$

which gives a T^5 behaviour at $T \ll \theta$ (where the integral becomes a constant), and the well-known linearity in T at high temperature. Here θ, or θ_D, is the Debye temperature which ranges from 100 K in potassium to 430 K in aluminium.
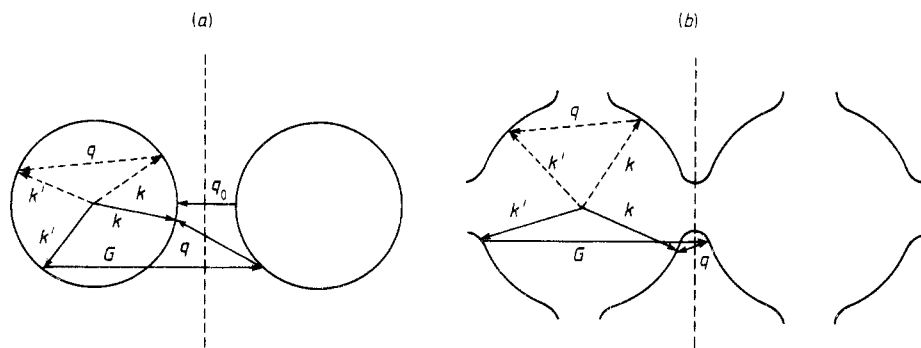
Figure 5. Momentum vectors involved in normal (broken lines) and Umklapp (full lines) electron-phonon scattering processes. (*a*) On an alkali metal Fermi surface. The minimum phonon momentum needed is represented by q_0. (*b*) On a polyvalent metal Fermi surface. There is clearly no minimum phonon momentum required in this case.

However, even early measurements did not show a T^5 term. A dependence slower than T^5 was to be expected when the sample was not far enough in the low-temperature limit, and was usually seen in the polyvalent metals. But in the 1950s, it was observed that $\rho(T)$ of sodium decreased faster than T^5 at the low T end. Measurements on potassium by Ekin and Maxfield (1971) and Gugan (1971) revealed a decay approximately exponential in T^{-1} down to about 2.5 K. The magnitude of $\rho(T)$ depended slightly on the impurity content of their samples. In the polyvalent metals, where $\rho(T)$ was found to follow approximately a power law, much more dramatic DMR from impurities were seen, leading to extensive quantitative investigations (for reviews see, apart from Bass (1972), Cimberle *et al* (1974) and Bobel *et al* (1976)).

The first obvious correction to be made to the simplified Bloch model in order to remove the discrepancies was the inclusion of Umklapp processes, in which the phonon momentum q is replaced by $q + G$, where G is a reciprocal lattice vector:

$$k - k' = q + G.$$

As one sees in figure 5(*a*), this needs a phonon with minimum momentum q_{min} if the Fermi surface does not touch the Brillouin zone boundary. Since the availability of phonons with at least a momentum q_{min} is governed by a Boltzmann factor

$$\exp\left[-\epsilon(q_{min})/k_B T\right] \equiv \exp\left(-\theta/T\right) \qquad \text{with } \theta \equiv \epsilon(q_{min})/k_B$$

such a factor also appears in ρ_{e-p}^U, multiplied by a scattering probability with a temperature dependence which is much more difficult to calculate for Umklapp than for normal processes. It is usually some low power law, and the exponential decay at low T is the dominant feature.

One more important difference between N and U scattering is that at low T, normal scattering produces only small differences in velocity v except where the Fermi surface is strongly curved (e.g. at Brillouin zone boundaries) whereas Umklapp processes cause v to change radically, thus decreasing the conductivity much more effectively.

Since no minimum wavevector is needed in the polyvalent metals Umklapp scattering persists and was expected to be relatively effective to the lowest temperatures: Lawrence and Wilkins (1972) found a T^5 term at very low T, and a lower power law at somewhat higher temperatures.

The effects of Umklapp scattering on $\rho_{e-p}(T)$ in simple metals were already included into calculations by Bailyn (1960). He also built some realistic features of the phonons into his model, allowing for some anisotropy. Since then, improvements became possible by various new techniques.

The relative importance of Umklapp scattering was studied by many authors, who showed that it is always predominant, also in the alkali metals at not too low temperatures. Thus, for example, Ekin (1971), Black (1972) and Trofimenkoff and Ekin (1971) gave an order of 60% as the Umklapp part of ρ_{e-p} where Pinchuk (1976) gets about 90% at 6 K for potassium. Detailed information about the phonon dispersion relations became available from experiment, mainly by inelastic neutron scattering (Cowley *et al* 1966, Meyer *et al* 1976). On the basis of these, Dynes and Carbotte (1968), for example, could calculate the ideal resistivity at higher temperatures; calculations of the difference between resistivity at constant volume and at constant pressure became possible (Hayman and Carbotte 1971, Kaveh and Wiser 1972a, b), as well as calculations of the volume dependence of $\rho(T)$ (Yamashita 1982). On the other hand, the theorist's ability to calculate these phonon spectra from first principles steadily increased to the point where the experimental data are very well reproduced, at least at zero pressure (e.g. Cowley *et al* 1966, Taylor and Glyde 1976; see figure 6).
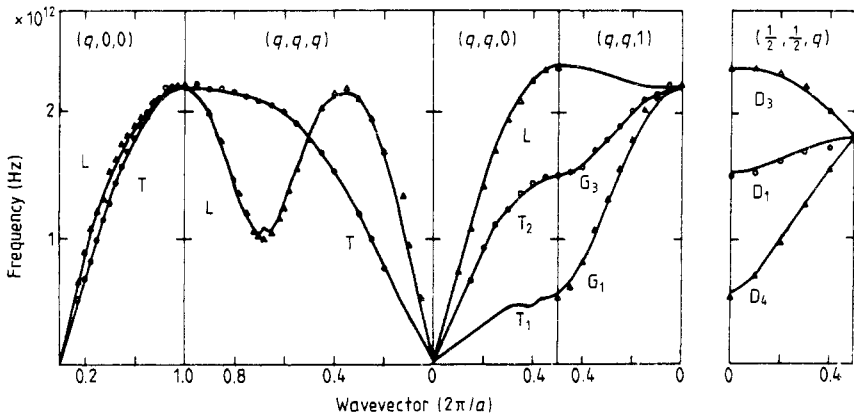
Figure 6. Phonon dispersion relations of potassium: calculations by Taylor and Glyde (1976) (full curves); symbols show data measured by Cowley *et al* (1966).

An important technique is the use of pseudopotentials which describe the interaction between an ion and its surroundings in a piece of metal. These can be of a local type like the Heine–Abarenkov potential or improvements on it (Srivastava and Singh 1976), which give satisfactory results in many cases, but the best accuracy is attained for most metals when using a non-local pseudopotential (see, for example, Dagens *et al* 1975). For an overview of how ρ_{e-p} is calculated from first principles see Taylor (1982). At temperatures $T > \theta_D/20$ these calculations are in satisfactory agreement with experiment now (see, for Na and K, Shukla and Taylor (1976) and Taylor *et al* (1976); for Rb and Cs, Taylor and MacDonald (1980)).

The importance of anisotropy in $\tau(k)$, and hence in the electron distribution function $f(k)$, gained attention because much of the observed DMR could be explained on this basis. Kagan and Zhernov (1971) pointed out that Umklapp scattering gives rise to a significant anisotropy in all metals. Isotropic scattering by impurities tends to isotropise

$f(\mathbf{k})$, thus bringing electrons into regions where the chance to be scattered by phonons is larger again: this makes $\rho_{\text{e-p}}(T)$ increase with the impurity content. A more quantitative study was undertaken by Ekin and Bringer (1973), especially for potassium. Their conclusion was that DMR resulting from isotropisation by impurity scattering would amount to some 12% of $\rho(T)$ at 4 K (assuming that $\tau(\mathbf{k})$ is completely isotropic because of the impurities; this means that the total effect of anisotropy is 12%). For the polyvalent metals much bigger effects were expected because Umklapp scattering is always effective in decreasing $\tau(\mathbf{k})$ close to the Bragg planes.

Calculations for potassium and aluminium by the diffusion model using these ideas (Lawrence 1975) gave similar results. Bobel *et al* (1976) argued, however, that DMR in metals should be considered at the same T/θ_{D}. In this way, DMR from impurities in potassium are of the same order of magnitude as that for polyvalent metals at low temperatures (<5 K). This view was at variance with theoretical insights of the moment, unless DMR from phonon drag quenching (see below) were taken into account.

It was shown by Leavens (1977) that it is necessary to account for the energy dependence of τ in the case of potassium in the lowest temperature range, e.g. at 6 K this lowered $\rho_{\text{e-p}}$ by 20%, in agreement with experiment. This improvement was combined with anisotropy in τ by Jumper and Lawrence (1977) who were able to explain much of the observed DMR in potassium in this way.

2.3.2. Phonon drag in the alkali metals. At low enough temperatures the Umklapp resistivity, decreasing exponentially, should become less than the normal scattering resistivity so that the Bloch T^5 dependence would be expected to be seen. The lowest temperature measurements of $\rho_{\text{e-p}}(T)$ by Gugan (1971) showed only an exponential term, suggesting that the Umklapp to normal scattering ratio at the lowest T was much larger than was explained by the present theories. A mechanism that could be responsible for this, phonon drag, had already been mentioned by Bailyn (1958), but it was assumed to be absent in the electrical resistivity by theorists at that time.

The phonon drag mechanism involves the inability of the phonon system to lose the momentum they acquire from the electrons. Phonon–phonon normal scattering was shown to be ineffective in this sense because of the Peierls condition by Roy (1974) and Kaveh (1977); Kaveh and Wiser (1979) also argued that phonon-dislocation scattering cannot restore the phonon system completely to thermal equilibrium. Thus, in the presence of an electronic current, the phonon system will be shifted in momentum space with a mean momentum equal to the mean electron moment, making normal processes ineffective in decreasing the current. In figure 2 we show the measured $\rho_{\text{e-p}}$ of potassium samples (van Kempen *et al* 1981) plotted semi-logarithmically as a function of T^{-1}. This graph demonstrates that indeed only an exponential term is present until below about 2 K the electron–electron term starts to dominate it.

A detailed calculation involves solving the coupled Boltzmann equations for the electron and phonon system. Kaveh and Wiser (1972b) concluded that the remaining Umklapp term of $\rho_{\text{e-p}}$ has the form:

$$\rho_{\text{e-p}}(T) \propto T^{-1} \exp(-\theta/T).$$

A precise prediction for the T exponent is a less simple matter, for example in the low-temperature limit, Kaveh and Wiser (1974a) predict a T^2 factor, Orlov (1975) a factor of T and Froböse (1977), taking the role of high frequency phonons into account,

predicts

$$\rho_{\text{e-p}}(T) \propto \left(\frac{T}{\theta}\right)^{3/2} \left(1 + B\frac{T}{\theta}\right) \exp\left(-\theta/T\right).$$

Only very precise experiments can discriminate between these different expressions. This is not very remarkable since in the temperature region of interest (3–6 K) functions of the form

$$T^n \exp\left(-\theta/T\right)$$

all look about the same when, together with n, θ is changed according to $\Delta\theta/\Delta n = -3$ K (Gugan 1971, Kaveh and Wiser 1979). The presence of phonon drag in the experimental data of Gugan (1971) and Ekin and Maxfield (1971) was postulated by Kaveh and Wiser (1974c) who found that with $n = 0$, $\theta = 23$ K. From high precision experimental data van Kempen *et al* (1981 figure 5) concluded that $n = 1$ is the optimum value together with $\theta = 19.9$ K. This is confirmed by various other experimental groups; now that one is sufficiently sure about what electron–electron term to subtract (see next subsection), the exponential behaviour can be seen (figure 2) to be valid down to about 1.3 K. This conflicts with the claim of Kaveh *et al* (1979) that θ cannot be assumed to be constant below 2 K.

After phonon drag was proposed, it was incorporated into many calculations (e.g. Hayman and Carbotte 1973, Roy 1974, Kaveh and Wiser 1974a, b, Leavens and Laubitz 1974, 1975). A discrepancy was visible between results for $\rho_{\text{e-p}}$(phonon drag)/$\rho_{\text{e-p}}$(no phonon drag) calculated by the Ziman one-iteration approximation to the Boltzmann equation (e.g. Hayman and Carbotte 1973) and those calculated via the variational method with a simple trial function (e.g. Ekin and Bringer 1973), the latter arriving at a much lower value at higher temperatures than expected from the 'exact' formalism from Bailyn (1958) as used by Kaveh and Wiser. Leavens and Laubitz tried to get out of this problem by iterating the Boltzmann equation until convergence, and concluded that the variational result prevailed over the one-iteration method because the latter would introduce an unphysically large electron distribution anisotropy. Calculations by Taylor *et al* (1976), comparing the situations with and without phonon drag, lead even to the conclusion that phonon drag was probably absent because the corresponding resistivity was much lower than data from experiment. Kaveh and Wiser (1977) questioned the validity of the form factor he used, however. Nevertheless Taylor (1978) defended his calculations by demonstrating the importance of phonon–dislocation scattering as a means of equilibrating the phonon system.

2.3.3. Sample dependence of $\rho_{\text{e-p}}$ in the alkali metals. In most high precision data of annealed samples, the electron–phonon term has been found to vary only a little in magnitude, and not at all in temperature dependence. However, a very puzzling set of data has been obtained from sample 3a of van Kempen *et al* (1981) which has a very high residual resistance, 186 pΩ m: this is about ten times the 'usual' value. This relatively fast cooled sample shows also a very high $\rho_{\text{e-p}}$. If one assumes the electron–electron term to be sample-independent (which will prove to be very questionable, see the next subsection) the ratio of $\rho_{\text{e-p}}$(sample 3a) to $\rho_{\text{e-p}}$(well-annealed samples) appears to explode below 3 K. In order to explain this feature, Danino *et al* (1981a, b) again invoked phonon–dislocation scattering, assuming a dislocation density of $n_{\text{d}} = 1.5 \times 10^{10}$ cm^{-2} for this sample: this was believed enough to bring the sample far out

of the phonon drag limit. This mechanism would cause the normal scattering T^5 term to partially reappear, so that it would predominate over the exponentially decaying Umklapp term below about 3 K. Gugan (1982) has demonstrated the improbability of such an n_d. Furthermore, even in the most highly dislocated sample K7-13 of van Vucht *et al* (1982), in which the dislocation density is relatively well known and cannot exceed 10^{10} cm^{-2}, the electron-phonon term is enhanced by a factor of two, but still behaves exponentially over the whole range down to 1.5 K. To obtain this result it is required that the electron-electron term is allowed to vary substantially in magnitude, but not in shape; the same applies to van Kempen's sample 3a. However, Haerle *et al* (1983) measured $\rho(T)$ of deformed potassium samples below 1.5 K and find that their data can be fitted better if they include a Bloch limit T^5 term.

Taylor *et al* (1978), believing that phonon drag is not necessarily present in the data, showed that phonon-dislocation scattering could also be responsible for the sample dependence of ρ_{e-p} in the data of van Kempen *et al* (1976), samples 2a, 2b and 2c. The validity of their calculation is, however, questioned by Kaveh and Wiser (1979).

Another model for the quenching of phonon drag involves anisotropic electron-dislocation scattering. Engquist (1982) has proposed a theory in which some low frequency phonons cannot return their momentum back to the electrons, so that phonon drag is partially suppressed. This permits the reappearance of the T^5 resistance in samples with high dislocation densities. He finds at least qualitative support for his results in the high precision data of Rowlands *et al* (1978).
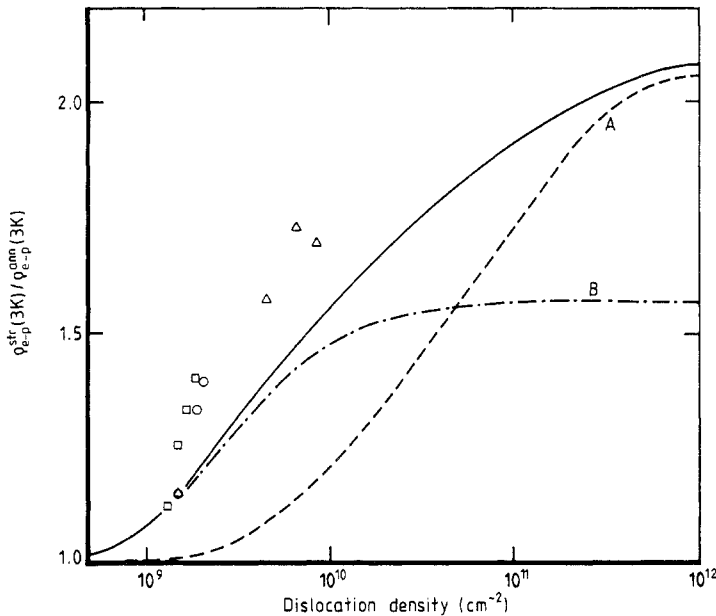
Figure 7. The ratio of the electron-phonon resistivities of strained and annealed potassium samples at 3 K as a function of the dislocation density calculated by Danino *et al* (1981b) for phonon drag quenching by phonon-dislocation scattering (A) and by Danino *et al* (1982) for phonon drag quenching by electron-dislocation scattering (B). The full curve shows the combined effect of both mechanisms. The symbols represent the values of $\rho_{e-p}^{str}/\rho_{e-p}^{ann}$ for samples of van Vucht *et al* (1982). The dislocation densities were inferred from the change in ρ_{e-e} after deformation (see § 2.3). ρ_{e-p}^{ann} was defined somewhat arbitrarily by requiring the annealed samples to lie on the predicted curve.

A similar theory, also involving an electron distribution made more anisotropic by dislocations, has been proposed by Danino *et al* (1982, 1983). It needs much smaller dislocation densities than the phonon–dislocation scattering theory to enhance ρ_{e-p} by factors up to 1.5. Here, data taken on strained and annealed samples by Gugan (1971) are used to demonstrate the ratio of $\rho(T)$(strained) to $\rho(T)$(annealed). When including a reasonable electron–electron term, the theory gives agreement with one of Gugan's samples. In contrast to what was found from samples 3a (van Kempen) and K7-13 (van Vucht), the strained to annealed ratio of ρ_{e-p} is predicted to be considerably temperature-dependent at low temperatures, however. On the other hand, the predictions agree qualitatively with the findings of Haerle *et al* (1983) for deformed potassium samples. This discrepancy has not been solved experimentally.

A combination of both mechanisms proposed by Danino *et al* (1983) is shown in figure 7. This figure gives the curves for $\rho_{e-p}^{str}/\rho_{e-p}^{ann}$ as a function of dislocation density at 3 K. We have added the values of $\rho_{e-p}^{str}/\rho_{e-p}^{ann}$ of some annealed and deformed samples of van Vucht *et al* (1982). In view of the crude assumptions that had to be made on the dislocation density of our samples, the agreement between the data and the combined theories is good.

2.3.4. The electron–phonon term in the polyvalent metals

2.3.4.1. Impurity dependence. The situation in the polyvalent metals is a little simplified because phonon drag is very unlikely to be found in them, as proved by Brody *et al* (1981). Far below the Debye temperature, one expects therefore a T^5 term from normal processes and T^4 or slower temperature dependence from Umklapp scattering. The latter would become relatively unimportant, however, at low T (Lawrence and Wilkins 1972). A pure T^5 behaviour was only seen in In (Wyder 1965); for aluminium and the noble metals powers between 3 and 4 were usually reported. In general the entire low-temperature region could not be described by a single power law (see, for example, Fickett (1971a,b) for a review of aluminium data, Rumbo (1976) for Cu and Ag, Barber and Caplin (1975) for Ag, Caplin and Rizzuto (1970) and Senoussi and Campbell (1973) both finding T^3 for Al; Babić *et al* (1976) found that aluminium alloys showed the sum of a T^3 and a T^5 term, with the former varying with impurity concentration). Furthermore, the temperature dependence was nearly always strongly dependent on impurity content of the samples, indicating large DMR. Using the popular two-band model, which considers the Fermi surface as being divided in two regions with different relaxation times for the various scattering processes (see, for example, Cimberle *et al* 1974), Dosdale and Morgan (1974) calculated a $T^{3.5}$ shape of ρ_{e-p} for dilute aluminium alloys, in agreement with Caplin's measurements.

Recently Khoshnevisan *et al* (1979a, b) observed $\rho(T)$ to go like T^4 in the noble metals, but in their purest copper sample an important T^2 term became visible. Going to lower temperatures, Schroeder *et al* (1981) saw pure T^2 terms in Cu and Al, whereas Barnard *et al* (1981) see a T^2 term emerge in their data from silver samples after cold work. These results are explained by Bergmann *et al* (1980a) and Borchi and De Gennaro (1980) who show that most of the observed T^4 dependence in the noble metals may be the sum of the electron–phonon term and a T^2 term from electron–electron scattering. Thus, much of the observed differences in magnitude and T dependence between samples with different amounts of static scatterers can be explained by different changes in the magnitude alone of the electron–electron and electron–phonon terms, respectively.

Returning to the DMR of the electron–phonon term itself, there is one more problem to be mentioned, which has not yet been solved completely: the two-band model and other successful models in which the anisotropy of scattering times for different scattering processes is allowed to vary (e.g. Bergmann *et al* 1974) always predict the DMR to 'saturate' in the limit of dominant impurity scattering, i.e. where $\tau(k)$ is isotropic. The impurity content at which the impure limit sets in is temperature-dependent and is expected to be in the dilute alloy range at temperatures below about $\theta_D/20$. Nevertheless, saturation is never observed (see Cimberle *et al* (1974) and many others; even the very accurate measurements of Ribot *et al* (1981) show no evident saturation at 4.2 K).

A new treatment of the DMR in polyvalent metals by Kaveh and Wiser (1980b), which was completely evaluated for aluminium in Kaveh and Wiser (1980c), provides a way out for the last problem in the form of an extra interference term between electron–phonon and electron–impurity scattering, producing extra enhancement of $\rho(T)$ in the impurity content region where the saturation should be seen. A crucial role for explaining DMR is assigned in these papers to the regions where the Fermi surface intersects the Brillouin zone boundaries. Here, the electron velocity $v(k)$ is very small, which increases the electron–phonon scattering probability, and a small change in momentum can change the velocity direction drastically. Electrons scattered into these 'hot spots' are therefore practically eliminated as contributors to the current. Since impurities, with their isotropic scattering time, scatter relatively more electrons into these regions than out of them, they produce positive DMR. By including an energy- and k-dependent relaxation time, several plane waves, electron–electron scattering and this concept Bergmann *et al* (1982a) have been able to explain most features of the observed $\rho(T)$ and DMR in the noble metals.

2.3.4.2. Dislocation dependence. A new puzzling phenomenon emerged when several groups not only varied the impurity content of their polyvalent metal samples, but also the dislocation density by deforming them. They often observed an astonishing decrease in $\rho(T)$ upon deformation: negative DMR (Rowlands and Woods (1978), Barnard *et al* (1981), Steenwyk *et al* (1981) and in an annealing experiment Sinvani *et al* (1981a, b)). It is evident that one has to view dislocations in a different way from impurities and other isotropic scatterers in order to account for this phenomenon.

The basic idea to solve the problem was already proposed by Dugdale and Basinski (1967): the relaxation time of electron–dislocation scattering is anisotropic in a way which resembles $\tau_{e-p}(k)$. This idea is employed by Sinvani *et al* (1981a, b) and Bergmann *et al* (1980b, 1981, 1982b) to explain the recent negative DMR. The argument uses the variational principle that requires $\tau_{e-disl}(k)$ to be such that ρ_{e-disl} is minimal. This produces a substantial decrease of τ_{e-disl} in the 'hot spots', making electron–dislocation scattering resemble electron–phonon scattering as opposed to electron–impurity scattering. When comparing samples of different polyvalent metals under similar conditions at the same temperature, differences in sign and magnitude of the DMR are found. These can be explained by a difference in effective temperature T/θ_D. In principle, this newest issue has also been solved by the theory of Bergmann *et al*; for example Steenwyk *et al* (1981) have been able to explain previous data taken by Khoshnevisan *et al* (1979a, b) and new data on impure and strained noble metal samples in the light of this theory.

2.4. Electron-electron scattering

2.4.1. Normal and Umklapp electron-electron scattering.
The belief that there should be an electron-electron resistivity term present in metals is much older than the actual observation of such a term in many metals. This resistivity contribution was, from the beginning, predicted to vary with T^2 (Landau and Pomeranchuk 1936). In order to understand such a temperature dependence, and the more recent developments on the magnitude of ρ_{e-e}, it is necessary to take a closer look at the Boltzmann equation mechanism for ρ_{e-e}.

One starts off from the equilibrium state density in k space:

$$f^0(k) = \frac{1}{1 + \exp\{[\epsilon(k) - \mu]/k_B T\}}.$$

Deviations from this equilibrium distribution, caused by an external electrical or thermal field, are considered to first order and characterised by a deviation function Φ:

$$f(k) = f^0(k) - \Phi(k)\frac{\partial f(k)}{\partial \epsilon(k)}.$$

The linearised BTE then reads:

$$-eV(k) \cdot E \frac{\partial f(k)}{\partial \epsilon(k)} = P\Phi(k) \tag{2.1}$$

where P is an operator representing scattering events; it can be approximated by

$$P \propto 1/\tau(k). \tag{2.2}$$

The resistivity follows from the variational principle as

$$\rho(T) = \text{constant} \times \langle \Phi, P\Phi \rangle$$

and is therefore easily seen to be inversely proportional to τ, which may represent the influence of several scattering processes. Ziman (1960) gives the complete expression for $\langle \Phi, P\Phi \rangle$. It looks like the following:

$$\langle \Phi, P\Phi \rangle \propto \frac{1}{\tau} \int dk_1 \int dk_2 \int dk_3 \int dk_4 (\Phi(k_1) + \Phi(k_2) - \Phi(k_3) - \Phi(k_4))^2 P_{1;2}^{3;4}. \tag{2.3}$$

Here $P_{1;2}^{3;4}$, the transition probability from states k_1, k_2 to states k_3, k_4 of the two electrons being scattered by each other, is composed of the Fourier transform of the screened Coulomb potential:

$$V(k, k') \propto \frac{1}{(k - k')^2 + q^2}$$

where $1/q$ is the screening length, and factors concerning momentum conservation:

$$\delta(k_1 + k_2 - k_3 - k_4)$$

for normal scattering, or

$$\delta(k_1 + k_2 - k_3 - k_4 + G)$$

for Umklapp scattering; G is a reciprocal lattice vector. These factors are temperature-independent. Note that the difference between electron-electron Umklapp scattering,

mostly a geometrical effect, and electron–phonon Umklapp scattering is that the latter 'needs' the availability of phonons with a minimal momentum, thus bringing in an extra temperature-dependent factor.

Furthermore, there is a factor for energy conservation, and the occupation numbers of original and final states, representing the Pauli principle which requires that the final states in the process must be unoccupied. The actual scattering rate is therefore governed by the number of final states that are available. At temperatures $T \ll \epsilon_F / k_B$, the Fermi–Dirac distribution function provides such states in a shell of thickness proportional to $k_B T$ around the Fermi surface. This fact contributes a factor T to the scattering rate τ_{e-e}^{-1}, and hence to the resistivity, for both electrons participating in the process. Until now, developments have mostly concerned the factor multiplying this T^2 term (at least at low temperatures), not the temperature dependence itself.

Important realistic calculations of the electron–electron resistivity were carried out by Lawrence and Wilkins (1973) for the alkali and simple polyvalent metals. The main point of interest was the relative importance of Umklapp scattering relative to normal scattering, expressed in their ratio Δ. This factor is of crucial interest, since normal isotropic scattering conserves the electron momentum and therefore makes no contribution to the resistivity. This can be seen by combining equations (2.1) and (2.2):

$$\Phi \propto \tau(\mathbf{k}) \mathbf{v}(\mathbf{k}) \cdot \hat{\mathbf{E}}.$$

Table 1. Calculated and measured values of Δ and A_{e-e} for simple metals: A_{e-e} is given in $10^{-16}\ \Omega\ \mathrm{m\ K^{-2}}$. The measured values of A_{e-e} are the highest and lowest values mentioned in the literature.

Metal	Δ^a	Δ^b	A^a	A^c	A^b Coulomb	A^b Phonon mediated	A (observed)
Li		2.4×10^{-3} [b]			0.6	21[b]	300[d]
Na	0.015[a]	1×10^{-5} [b]	1.5[a]	10[c]	0.1	14[b]	18–19.5[e]
K	0.06[a]	7×10^{6} [b]	17[a]	24[c]	0.4	17[b]	6–81[f]
Rb		1.3×10^{-3} [b]		43[c]	1.6	35[b]	?
Al	0.4[a]		1.2[a]		1.8	41[g]	27[h]–60[i]
In	0.4[a]		2.4[a]				550[p]
Cu	0.8[l]	(0.3–0.4[n])	7.6[l]		20	19[g]	1.4–5.9[m]
Ag	0.7[l]		14[l]		20	17[g]	3[k]–4.7[j]
Au	0.8[l]		14[l]		25	30[g]	4[k]–6.1[o]

[a] Lawrence and Wilkins (1973).
[b] MacDonald et al (1981).
[c] Awasthi and Sathish (1981).
[d] Sinvani et al (1981a), Yu et al (1983) at $T > 1$ K.
[e] Levy et al (1979).
[f] van Vucht et al (1982).
[g] MacDonald (1980).
[h] Ribot et al (1981).
[i] R J M van Vucht (unpublished).
[j] Khoshnevisan et al (1979a).
[k] Bergmann et al (1980a).
[l] Lawrence (1976).
[m] Steenwyk et al (1981).
[n] Black (1978).
[o] Borchi and De Gennaro (1980).
[p] Garland and Bowers (1969).

This makes the resistivity effectiveness factor from $\Phi(k)$ in equation (2.3) look like

$$[\tau(k_1)v(k_1) + \tau(k_2)v(k_2) - \tau(k_3)v(k_3) - \tau(k_4)v(k_4)]^2. \tag{2.4}$$

In the isotropic limit where $\tau(k)$ is a constant, and especially in the alkali metals where $v(k) \propto k$, this factor vanishes for normal scattering. Therefore, Δ essentially determines the magnitude of A_{e-e}. Since one plane wave suffices to describe the electron wavefunctions of most alkali metals, the Umklapp contribution to their resistivity is also rather small, i.e. Δ is of the order of a few per cent. Values calculated by Lawrence and Wilkins (1973), MacDonald *et al* (1981) and Lawrence (1976) for several simple metals can be found in table 1.

Using different pseudopotentials, screening lengths, etc, other estimates of Δ have been published by various authors. Especially interesting is the approach of Awasthi (1981) and Awasthi and Sathish (1981) who did not separate the resistivity into normal and Umklapp contributions, but rather took the lattice periodicity into account by means of an overlap integral involving the Bloch wavefunctions of electrons with their momenta separated by reciprocal lattice vectors. For potassium, they find a somewhat high value for A_{e-e}, but for sodium their result is reasonable.

2.4.2. Observation of T^2 terms

2.4.2.1. The alkali metals. In lithium, a T^2 behaviour of the resistivity up to 10 K was reported by Krill (1971). This result was later confirmed by measurements by Sinvani
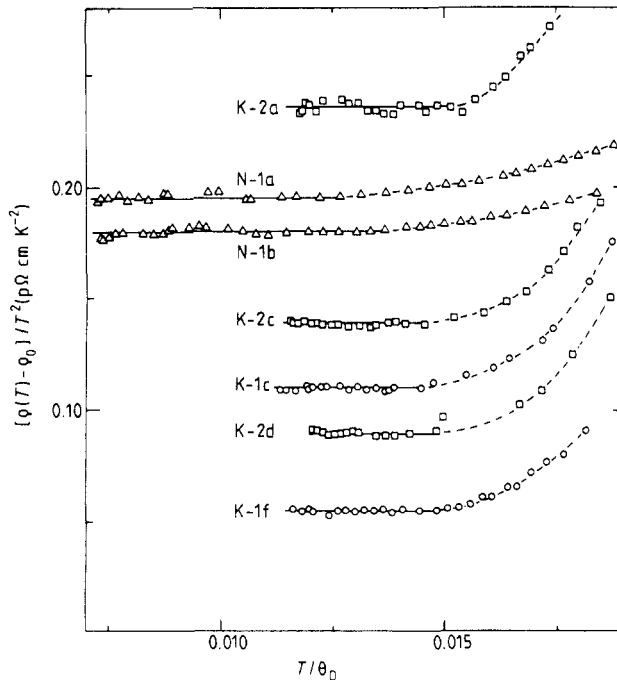
Figure 8. A plot of $(\rho - \rho_0)T^{-2}$ as a function of T for sodium and potassium samples (Levy *et al* 1979). The temperature is divided by the Debye temperature since the electron–phonon term in both metals starts becoming important at about the same relative temperature. The pure T^2 dependence which is attributed to electron–electron scattering is seen to dominate $\rho(T)$ over a temperature range sufficient to determine its magnitude.

et al (1981a, b). It took several years before the new experimental methods with greatly improved accuracy were able to show that such a term is also present in potassium (van Kempen *et al* 1976) which is, not very surprisingly, more than an order of magnitude smaller than in lithium and therefore hidden under the electron–phonon term down to about 1.4 K. Since they had to make assumptions on the electron–phonon term which was still controversial (Kaveh *et al* 1979), a better avenue to follow was to measure down to lower temperatures where ρ_{e-p} is negligible. Figure 8 shows such low-temperature measurements on potassium and sodium (Levy *et al* 1979). In this plot, the horizontal parts of the curves correspond to a pure T^2 behaviour.

Some controversy arose when Rowlands *et al* (1978), the first to carry out high precision measurements below 1.2 K, found that the resistivity of their (0.79 mm diameter) K samples behaved more like $T^{1.5}$ than like T^2. Later Lee *et al* (1982) measured $\rho(T)$ for a number of thicker samples and confirmed the existence of a T^2 term down to 0.4 K. By a Monte Carlo simulation, Black (1980) has shown that the sample size can be responsible for deviations from T^2 in thin samples. Very recently, Yu *et al* (1984) measured a series of samples with diameters ranging from 0.09 to 1.5 mm and indeed found important deviations from T^2 behaviour in samples thinner than 1 mm. Their interpretation invokes an effect proposed by Gurzhi (1963), involving interference between normal electron–electron scattering and surface scattering. Consequently, another explanation of Rowlands' data by Bishop and Overhauser (1979, 1981), based on electron–phason scattering in the presence of a charge density wave structure, lost its significance. One important feature of ρ_{e-e} in potassium remains the

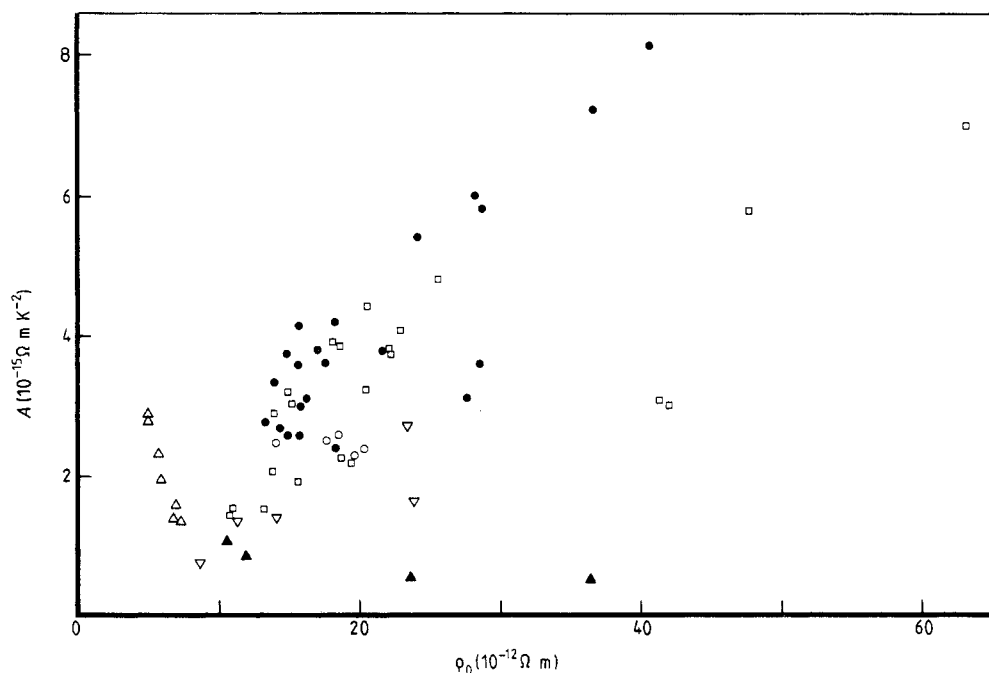**Figure 9.** The coefficient A_{e-e} for many potassium samples with largely different residual resistivities ρ_0. No systematic dependence is visible. The symbols represent measurements from: Levy *et al* (1979) ($\triangle$, $\blacktriangle$), van Kempen *et al* (1981) (∇), Lee *et al* (1982) ($\bigcirc$), Haerle *et al* (1983) ($\square$) and van Vucht *et al* (1982, unpublished) ($\bullet$).

unexpected sample dependence of its coefficient A_{e-e}. Figure 9 shows A_{e-e} for a large number of potassium samples from various authors, plotted as a function of ρ_0. There is clearly no simple relationship between these properties.

2.4.2.2. Aluminium. Garland and Bowers (1969) ascribed a T^2 term in aluminium and indium to electron-electron scattering. Senoussi and Campbell (1973) found T^3 for $\rho(T)$ of Al from 1.2 to 4.2 K. Kaveh and Wiser (1975a) interpreted this as the sum of an electron-phonon term and again a T^2 term from electron-electron scattering. High accuracy measurements on samples which had widely varying residual resistivity and which had undergone quite different treatments (van Kempen *et al* 1978, Ribot *et al* 1979, 1981) were entirely consistent with this picture, and showed an A_{e-e} constant to within 10% (figure 3). Ribot *et al* (1981) also argue why the T^2 term must certainly be ascribed to electron-electron scattering; other proposed mechanisms as found in § 2.4 could be ruled out. Finally, Schroeder *et al* (1981) measured $\rho(T)$ of Al down to 0.3 K in a small magnetic field and found the expected shape and magnitude (corrected for field dependence) over the whole temperature range.

The magnitude of A_{e-e} in all these observations was about a factor of 20 higher than the value predicted by Lawrence and Wilkins (1973), $1.2 \times 10^{-16} \, \Omega \, \text{m} \, \text{K}^{-2}$. Various improvements on their method of calculating ρ_{e-e} caused only by Coulomb scattering were of little help. Only recently, MacDonald (1980) showed that the discrepancy could be removed by taking the influence of the phonons into account; partly via an enhanced quasiparticle mass and partly via the phonon-mediated character of the interaction, the missing factor of 20 is resolved. A similar treatment for the alkali metals (MacDonald *et al* 1981) shows that the Coulomb scattering contribution in those metals must be much smaller than previously found, but the phonon-mediated interaction restores the old order of magnitude.

2.4.2.3. The noble metals. Lawrence (1976) demonstrated the appearance of an electron-electron scattering originated T^2 term in the data of Rumbo (1976) for the noble metals. Khoshnevisan *et al* (1979a) found that $\rho(T)$ of silver went generally like T^4 from 0.4-7 K, but at the lowest temperatures an indication of T^2 behaviour was observed. The same happened to copper, in which an approximate T^2 term was seen below 2 K (Khoshnevisan *et al* 1979b). Bergmann *et al* (1980a) claimed that a T^2 term was hidden in all the silver data of both Khoshnevisan *et al* and Barnard *et al* (1981, 1982). A pure T^2 behaviour was reported by Schroeder *et al* (1981) for copper at sufficiently low temperatures. Such a limiting region for silver was not found because of an extra effect showing up around 0.3 K, with similar features as in the potassium data of Lee *et al* (1982). The Debye temperature, which is lower in silver than in copper, makes the electron-phonon term important at considerably lower temperatures. In gold, the Debye temperature is even lower, so that there is little hope to observe a pure T^2 region. Nevertheless, the occurrence of a simple electron-electron scattering contribution to the resistivity of the noble metals cannot be denied any more.

2.4.3. Sample dependence of A_{e-e}

2.4.3.1. Explanation of the sample dependence from anisotropic scattering. The upper and lower limits of the measured A_{e-e} values in table 1 indicate the spread of A_{e-e} values among different samples of the same metal. This spread is an order of magnitude larger in potassium than in the simple polyvalent metals, and was therefore first observed in potassium (see, for example, van Kempen *et al* 1981).

Since such a sample dependence conflicts with the fundamental ideas underlying the calculation of A_{e-e} by, for example, Lawrence and Wilkins (1973), a way had to be found to introduce a non-intrinsic property, varying from sample to sample and affecting the magnitude of A_{e-e}. Kaveh and Wiser (1980a, 1982) argue that dislocations are the best candidates for this role. Dislocations, and other scattering centers like grain boundaries, and maybe even impurities (Llewellyn *et al* 1977a, b) or the sample surface, are expected to cause an anisotropic relaxation time. For dislocations, this is easy to imagine: the dislocation core can be viewed as a long charged region which is hardly experienced by electrons moving approximately parallel to it, but has much more effect on electrons which move in a plane perpendicular to it. Grain boundaries can be considered as dislocation arrays. Since the resistivity is determined by the factor (2.4), a deviation from a constant τ can increase the magnitude of the normal scattering contribution to ρ_{e-e} from zero to a considerable value. Now, $\tau(k)$ in (2.4) is just an average over *all* scattering mechanisms. At very low temperatures, the dominant scattering mechanisms are impurity scattering and dislocation scattering, so that the anisotropy in τ is coupled directly to the relative importance of the anisotropic part of these mechanisms. The residual resistivity ρ_0 is proportional to $\tau_0^{-1} = \tau_{iso}^{-1} + \tau_{ani}^{-1}$ and can thus be divided into ρ_{iso} and ρ_{ani}, which we shall call further on ρ_i and ρ_d. Here we have redefined the meaning of the subscripts i and d, which are traditionally used for impurity and dislocation scattering, respectively. Thus, $\rho_d(\rho_i + \rho_d)^{-1}$ is a measure of the anisotropy of τ.

Kaveh and Wiser calculate the enhancement of the normal and Umklapp electron–electron scattering rates with this ratio as a parameter and find

$$A_{e-e} = A_0 + A_1 \left(\frac{\rho_d}{\rho_d + \rho_i} \right)^2 \qquad (2.5)$$

where A_0 is the Umklapp contribution in the isotropic limit. A_1 corresponds to the maximum contribution from normal scattering. An estimate of A_1 is difficult because the anisotropy of the electron–dislocation scattering time is badly known. In fact, Kaveh and Wiser made such assumptions that the observed variation in potassium from sample to sample could be explained by assuming that only the dislocation content varied. Fitting their formula to data from van Kempen *et al* (1976), Rowlands *et al* (1978) and Levy *et al* (1979), they found that $A_1 = 3.5 \times 10^{-15} \, \Omega \, m \, K^{-2}$ (figure 10). This is to be compared to the expected value of A_{e-e} in the isotropic limit of about $0.5 \times 10^{-15} \, \Omega \, m \, K^{-2}$. The data of van Kempen *et al* (1981) for sample 3a, exhibiting both an anomalously large ρ_0 and A_{e-e}, led Danino *et al* (1981a) to conclude in the light of this result that this sample was in the anisotropic limit.

2.4.3.2. A_{e-e} of lithium. Lithium undergoes a martensitic transform in the vicinity of 75 K and can therefore be expected to show an abundance of dislocations when cooled below this temperature. According to the Kaveh and Wiser theory, this produces a considerable increase in A_{e-e}. Also, among the alkali metals the Fermi surface comes closest to the Bragg planes in lithium and is hence far more deformed from sphericity than, for example, in potassium. This necessitates the use of multiple plane waves to describe the electron wavefunctions. This also increases the Umklapp processes, though not enough to account for the large A_{e-e} completely (MacDonald *et al* (1981) find only about 10% of the experimental values by including Umklapp and phonon-mediated processes).
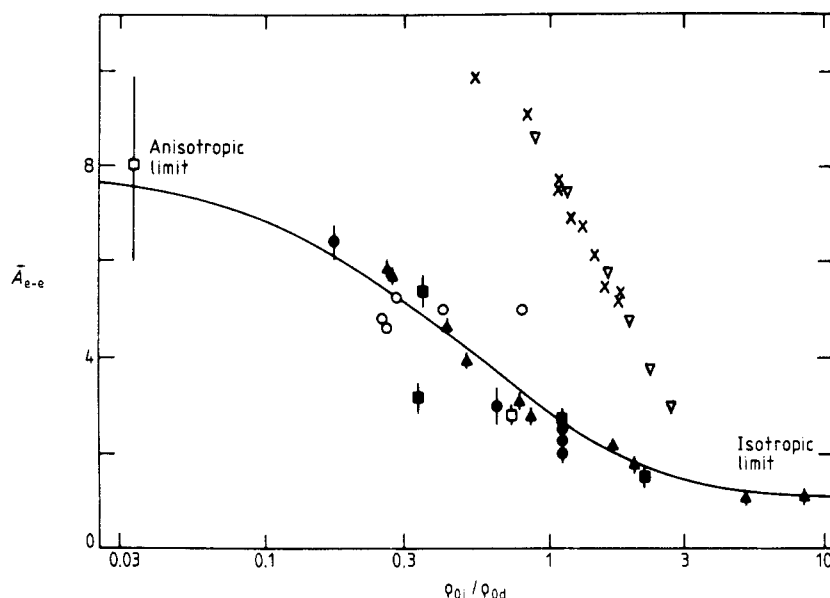
Figure 10. A_{e-e} of a large number of potassium samples from different authors plotted as a function of ρ_i/ρ_d to show the agreement with the theory of Kaveh and Wiser (1982). The data are scaled to the value of A_{e-e} in the isotropic limit. In the case of most symbols ρ_i and ρ_d were inferred by Kaveh and Wiser; for the crosses (samples of van Vucht *et al* (1982)) and open triangles (Haerle *et al* 1983) these numbers were extracted from a plot like figure 11. For the latter samples, a serious discrepancy with the original theoretical curve (full curve) is visible. This can be removed by increasing the magnitude of A_{e-e} in the anisotropic limit by a factor of about 5.

Indeed, A_{e-e} is an order of magnitude larger in lithium than in potassium (30 as against an average of $2.5 \times 10^{-15}\ \Omega\ m\ K^{-2}$) as measured by Krill (1971) and Sinvani *et al* (1981a, b), and recently by Yu *et al* (1983). The absence of sample dependence is conceivable since all samples will already be in the anisotropic limit. Thus, lithium offers strong evidence for the correctness of the idea behind the Kaveh and Wiser theory.

2.4.3.3. Systematic investigation of the sample dependence. Various groups set out to check the validity of equation (2.5) by changing either the impurity content or the dislocation density of their potassium samples stepwise, measuring $\rho(T)$ after each step.

Levy *et al* (1979) gave impurities the opportunity to diffuse into their potassium and sodium samples between subsequent runs. They assumed that the dislocation density, on the other hand, did not vary significantly upon each cool down. In this way, they obtained results which were even quantitatively in agreement with Kaveh and Wiser's predictions. In sodium, the decrease in A_{e-e} was relatively small, for the same reason as in lithium: a martensitic transformation causes a high dislocation density even in undeformed samples.

On the other hand, keeping their samples' impurity content constant, van Vucht *et al* (1982) deformed their wire samples by torsion at or below 4.2 K. It appears that the magnitude of the T^2 term increases considerably upon deformation. The analysis of these data showed that it was perfectly possible to describe the results using equation (2.5) over a considerable range of residual resistivities, but that a much (about 5 times) larger value for A_1 emerged (figure 10); a maximum value of $8.1 \times 10^{-15}\ \Omega\ m\ K^{-2}$ was

measured. It was found that A_0 could be considered negligible with respect to the second term in (2.5). Annealing experiments showed not only that dislocations played a role in the anisotropic part of τ, but also probably another extended defect which anneals out at very low temperatures, identified by the authors with long vacancy pipes.

The apparent contradiction with the results of Levy *et al* (1979) can be removed by assuming only a higher ρ_d for their samples than they did. The fact that their data lie on about a constant $\rho_0\sqrt{A_{e-e}}$ value (which corresponds to $\rho_d\sqrt{A_1}$ according to equation (2.5)) in figure 11 confirms however that ρ_d did not vary much from sample to sample. Thus, the effect of dislocations on anisotropy of τ may be much more pronounced than Kaveh and Wiser used to fit their model.
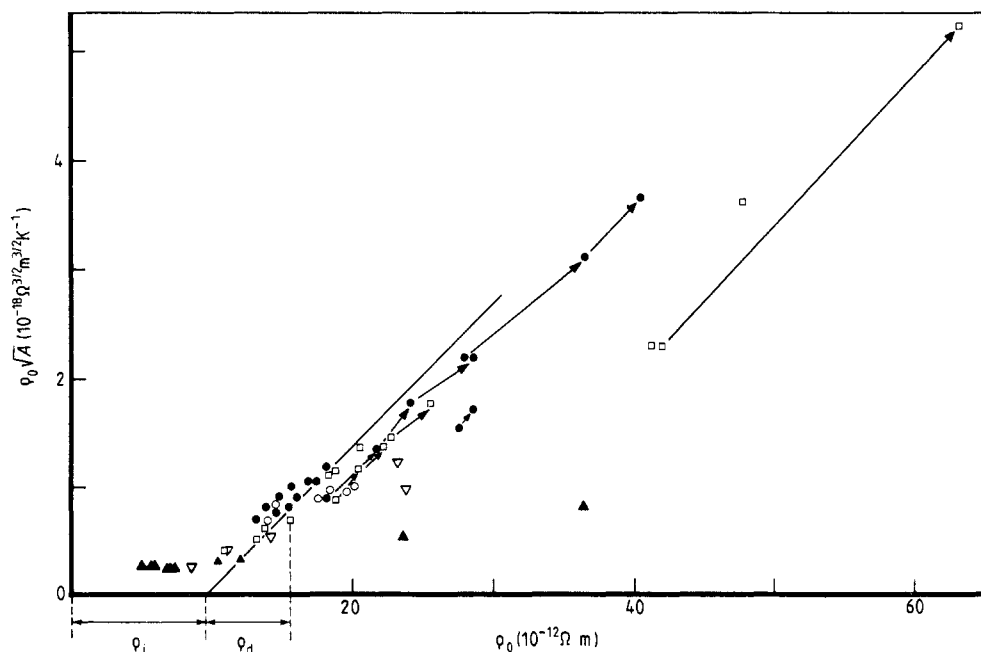

Figure 11. $\rho_0\sqrt{A_{e-e}}$ plotted as a function of ρ_0 for a large number of potassium samples from different authors. Data of the same sample after different stages of deformation are linked with arrows. The theory of Kaveh and Wiser predicts that if only ρ_d varies the data lie on a straight line with slope $\sqrt{A_1}$ and intercept ρ_i with the ρ_0 axis. All data of van Vucht *et al* (1982) (full circles) and Haerle *et al* (1983) (open squares) are approximately consistent with this theory and give an A_1 of about $190 \pm 20 \times 10^{-16} \ \Omega \ \mathrm{m \ K^{-2}}$ for most data. When a specific A_1 is assumed this plot enables one to determine the ρ_d part of ρ_0 from A_{e-e}. Open triangles are from van Kempen *et al* (1981); closed triangles from Levy *et al* (1979); open circles from Lee *et al* (1982).

The Michigan group chose to deform potassium by squeezing their samples between two flat plates; their measurements extend down to 0.1 K (Haerle *et al* 1983). When viewed above 1 K (the temperature range to which the other groups are confined), their data are consistent with A_{e-e} increasing on increasing ρ_d. Below 1 K, however, an unexpected change in the temperature dependence of $\rho(T)$ troubles the picture (figure 12). This change is tentatively ascribed to an extra term from scattering of electrons by vibrating dislocations, proposed by Gantmakher and Kulesko (1975). Such a behaviour is in agreement with the experimental fact that the low-temperature anomaly increases sharply with increasing dislocation content, and decreases upon
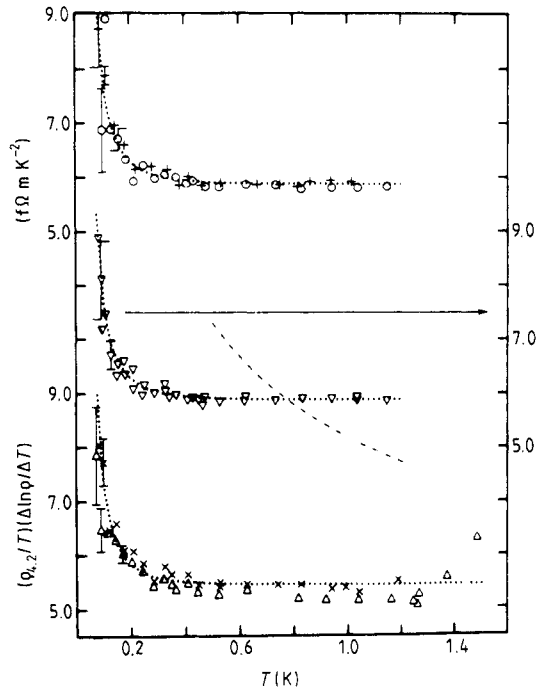
Figure 12. Scaled values of $d\rho/\rho T\,dT$ as a function of T below 1.4 K for potassium samples (Lee *et al* 1982) showing the anomalous increase from the expected constant value at low T. Apart from being seen as an increase in A_{e-e}, this phenomenon can be ascribed to an extra term, probably from inelastic electron–dislocation scattering.

annealing so that it cannot be caused by the change in geometry after squeezing. This extra term extends to higher temperatures where its effect can be mistaken for an increase in the T^2 term. Therefore it may be necessary to reinterpret the data of the other groups if this nature of the anomaly is confirmed by further experiments.

Another possibility that should not be overlooked, however, is that it is really A_{e-e} that varies with temperature because of the eventual variation with temperature of the anisotropy caused by electron scattering from certain entities. Since vibration modes of self-interstitials, interstitial impurities or dislocations freeze out at specific temperatures, these may be much more anisotropic as seen by the electrons than at temperatures where their vibrational modes are mostly excited.

An anomaly of the same kind has already been observed in undeformed silver crystals (Schroeder *et al* 1981) and has recently been shown to be very pronounced in undeformed lithium and rubidium samples (Yu *et al* 1983).

2.4.3.4. Sample dependence of A_{e-e} in the polyvalent metals. Whereas the Kaveh and Wiser theory on the sample dependence of A_{e-e} was devised originally for the alkali metals, the same effect has been observed in deformed samples of aluminium and copper. The observed variations are slightly less impressive than in potassium, because Umklapp scattering is relatively more important in these metals with Fermi surfaces crossing the Brillouin zone boundaries.

Sinvani *et al* (1981a, b) first measured $\rho(T)$ of deformed aluminium samples, annealed them and then measured $\rho(T)$ again. The samples were not very pure and

thus went from a somewhat anisotropic situation into the isotropic limit. The electron-phonon term increased thereby (see § 2.2), but at the same time A_{e-e} decreased by about 20%. The magnitude of this decrease, as well as the sample to sample variation of A_{e-e} in the data of, for example, Ribot *et al* (1981) of some 15%, can be understood in terms of a Δ of about 0.4, permitting a maximum enhancement of A_{e-e} by about 2.5 times.

A sharp increase in A_{e-e} has also been seen in copper and copper–silver alloys by Steenwyk *et al* (1981) and Zwart *et al* (1983), and the data of several previous authors on silver and copper have been analysed in view of electron–electron scattering enhancement by Bergmann *et al* (1980a, 1982a, b). Steenwyk's data on copper have been explicitly shown to be in quantitative agreement with this theory by Kaveh and Wiser (1983a, b) based on the calculated value of Δ of 0.3–0.4. Since the maximum value of Δ is, of course, 1 this implies, as in aluminium, a maximum variation in A_{e-e} of about a factor of 3.

2.4.3.5. Temperature dependence of A_{e-e}. The Kaveh and Wiser (1981a) theory and MacDonald's phonon-enhanced electron–electron scattering theory together explain the different behaviour of A_{e-e} at low and high temperatures in the alkali metals, in aluminium and in the noble metals. Since at high temperatures ($T \gg \theta_D/5$) electron–phonon scattering dominates and is very isotropic, all sample dependence in A_{e-e} found in potassium at low temperatures disappears. In aluminium, A_{e-e} decreases at higher temperatures since the phonon-mediated contribution disappears, and in the noble metals, where this contribution is not important, A_{e-e} remains about constant.

2.5. Other temperature-dependent terms

Apart from electron–phonon, electron–electron and electron–vibrating-dislocation scattering, a few other temperature-dependent resistivity contributions are proposed for simple metals. Some of these have T^2 behaviour and can thus be mistaken for electron–electron scattering effects, or vice versa.

2.5.1. Surface scattering. When the bulk electron mean free path is of the same order of magnitude as the sample dimensions, i.e. when the latter are comparable to or smaller than about a millimetre for pure metals at low temperatures, a considerable fraction of the collisions that a conduction electron undergoes is on the sample surface. Apart from reducing the mean free path directly (a temperature-independent process), this can cause DMR by interference of surface scattering and electron–phonon or electron–electron scattering.

A heuristic prediction of a T^2 term from surface scattering is proposed by van der Maas *et al* (1981, 1983) who base this on an analysis of existing data. The samples involved have much smaller dimensions than those used in most experiments mentioned above, so that their T^2 term cannot be entirely caused by this size effect. On the other hand, the surface may be seen as one giant anisotropic scatterer and therefore causes the electron–electron term to be raised by over a factor of 2–5 in the polyvalent metals. The order of magnitude of the observed variations in the noble metals is in agreement with such a point of view.

Note, however, that the size-dependent effects recently observed by Yu *et al* (1984) show serious deviations from T^2 behaviour. Since this effect occurs below 1 K, and the van der Maas analysis applies at higher temperatures, there is no direct discrepancy.

Sambles and Preist (1982) performed an extensive calculation of the effects of surface scattering on $\rho(T)$ and found that this influence may consist both in the enhancement of a T^2 term in $\rho(T)$ of the bulk metal and in the appearance of an extra T^2 term due to electron-phonon scattering. There is a lack of systematic data to test this theory quantitatively so far.

Furthermore, there is the Gurzhi effect mentioned above, which is invoked by Yu *et al* (1984) to explain their results qualitatively.

Since the effects of surface scattering are apparently not well understood at this time, precision measurements of $\rho(T)$ for bulk metals should be performed on samples with diameter greater than 1 mm.

2.5.2. Inelastic impurity scattering. In the 1960s, Koshino (1960, 1963) and Taylor (1964) found evidence that inelastic electron-impurity scattering should contribute a T^2 term to the resistivity. Such a term was reported for potassium containing rubidium impurities by Lee *et al* (1980). It is recognised by the linear variation of its magnitude with the Rb concentration. For samples with impurity content up to about 0.1%, it is comparable to the electron-electron term. Therefore it is tempting to interpret at least part of this term also in terms of modification of the electron-electron term because of the anisotropy of electron-Rb-impurity scattering, which is shown to be considerable by Llewellyn *et al* (1977a). However, the linearity in concentration and the lack of saturation of this term, which would be prescribed by equation (2.5), show that this effect cannot be exclusively responsible for the observed large T^2 terms.

A T^2 term from electron-vibrating-impurity scattering was also proposed by Kagan and Zhernov (1966), who found at the same time that impurities could also give rise to T^4 and T^5 terms by modifying electron-phonon scattering.

New calculations by Fleurov *et al* (1980) predict even a negative $\sqrt{T}$ term from interference between electron-electron and electron-impurity scattering, which would be replaced at somewhat higher T by a T^2 behaviour, and therefore gives rise to a resistance minimum. Experimental evidence for such a term is lacking, however. Also, a danger would exist in confusing this term with the Kondo term arising from magnetic impurities, which is well known to produce a resistance minimum, too.

2.5.3. Temperature-dependent terms from electron-dislocation scattering. Measurements on copper and molybdenum samples showing steeply rising temperature-dependent terms with a magnitude proportional to dislocation density led Gantamakher and Kulesko (1975) to propose two mechanisms explaining such a behaviour from electron scattering on dislocations. In the first mechanims, the electron scattering is influenced by vibration energy levels of the dislocations. These authors prefer a mechanism in which the scattering is caused by the existence of levels closely above the Fermi surface in the vicinity of dislocations, and are able to fit their measurements to a formula derived for this situation. Measurements on gold supporting this theory have also been reported by Endo and Kino (1979). The Michigan State University group was also reasonably successful in fitting their data (showing the low-temperature anomaly) to the vibrating dislocation theory. However, the values of the involved parameters are quite different for both experiments, the temperatures being of the order of 100 K for the data of Gantmakher and Kulesko as opposed to 0.1 K for the data of Lee *et al* (1980), and the magnitudes being very different. Such discrepancies may be caused by the quite different nature of the metals considered, but it is more likely that different processes are involved.

2.6. More DMR sources

An appreciable part of the previous subsections has described deviations from Matthiessen's rule, mostly caused by interference between different scattering processes, and sometimes by new scattering mechanisms related to sample-dependent properties. We shall now cover a few effects which have not already been mentioned.

The temperature-dependent resistivity of lithium samples in which two isotopes were present in varying relative amounts was measured by Babushkina *et al* (1982). DMR in these crystals were explained not only from isotropisation of the scattering time, but also from deformation of the phonon spectrum caused by the differences in ionic masses.

A high magnetic field was used in measurements on aluminium samples as an additional way of moving electrons across the Fermi surface over such large angles that the effect was to isotropise the electron distribution (Mitchel *et al* 1980). In this way, in fact, a decrease of the DMR caused by impurities was obtained. This supports theories which explain DMR in zero field from anisotropic electron–phonon scattering.

2.7. The residual resistivity

The residual resistivity, or resistivity at (extrapolated to) $T = 0$ K, is by far the dominant term at low temperatures for even the purest metals. Therefore, originating from the idea that it arose only from impurities, metals are still said to be in the 'impure limit' below, say, a few tens of K. Of course, apart from impurities many different structural defects also contribute to the residual resistivity in widely varying degrees. In view of the previous subsections, where it was pointed out that impurities and lattice defects may have completely different influences on $\tau(k)$ and therefore on DMR in the temperature-dependent terms, it is clearly essential to have as detailed a knowledge and/or control as possible for the relative amounts of each scatterer in the samples.

2.7.1. Electron–impurity scattering.

A very complete review by Aleksandrov (1971) on contributions to ρ_0 demonstrates that the residual resistivities of even the purest metals are indeed dominated by impurities as long as they are properly annealed. The purest metal samples available today have impurity concentrations down to 1 part in 10^9, giving residual resistance ratios $(=\rho(273 \text{ K})/\rho_0)$ of more than 10^5; typical numbers are a factor of 10–50 worse for the polyvalent metals and a factor of 50–500 worse for the alkali metals. Most impurities are either metals, carbon, hydrogen, nitrogen or oxygen. Ferromagnetic metal impurities form an especially awkward problem for the study of $\rho(T)$ of the noble metals where they give rise to an important Kondo effect if present in measurable quantities. A tabulation of the contribution of different impurities to the residual resistivity can be found in Bass (1982).

Most impurities occupy lattice sites and are usually assumed to be isotropic scattering sources for the conduction electrons. It was found by Llewellyn *et al* (1977a) from Dingle temperature measurements as a function of the orientation of potassium crystals that there is an anisotropy of 10.8% in the scattering time from rubidium impurities, however, and of 19.5% from sodium impurities. These results show that, at least in the alkali metals, impurities should not be regarded as completely isotropic scatterers. An explanation of the anisotropy (Llewellyn *et al* 1977b) involves variations in electron wavefunctions over the Fermi surface and the anisotropy of strain introduced in the lattice.

2.7.2. Lattice defects. Lattice defects are usually divided into two groups according to their spatial character: on the one hand, vacancies and self-interstitials which are point defects (though around which the lattice is a little deformed), and on the other hand extended defects like dislocations, stacking faults and grain boundaries. The limits are vague since vacancies and interstitials are known to form certain complexes extending over several lattice constants, and dislocations can form very small loops of about the same size. However, considering the influence on transport, the division into point defects and extended defects is convenient.

2.7.3. Annealed samples. There is always some minimum number of lattice defects present, even in well-annealed samples. At higher temperatures, this is caused by the defects being in thermal equilibrium with the lattice. This effect is appreciable only when the defect formation energy is close to kT, i.e. in practice only for vacancies and self-interstitials at temperatures of the order of the melting temperature. At lower temperatures, their concentration dies away exponentially if one cools the samples infinitely slowly. Since this is never possible, very small concentrations, usually masked by impurities, always persist. To study imperfections other than impurities, one can use quenching from a certain temperature to obtain a sample with a high point defect density which reflects the density at that temperature.

A remanent dislocation density in well-annealed alkali metal crystals is measurable by x-ray techniques. These dislocations form a mosaic block structure with a density of about $10^6 \, \text{cm}^{-2}$ (Adlhart *et al* 1981). Also, Gugan (1982) asserts that a dislocation density of $10^7 \, \text{cm}^{-2}$ is the highest reasonable density for an annealed potassium sample. The residual resistance due to these dislocations is immeasurably low even for the purest available metals.

The same applies to grain boundaries in non-single crystals as long as the crystallites are of the order of typical sample dimensions like 1 mm or so. For a few polyvalent metals, Aleksandrov *et al* (1974) found a resistivity contribution from grain boundaries ρ_{gb}/n_{gb} of about $10^{-11} \, \Omega \, \text{cm}^2$. Using distances between them of 1 mm, this gives $10^{-10} \, \Omega \, \text{cm}$, which is low with respect to ρ_0 from impurities.

2.7.4. Deformed samples. Samples are deformed mostly by tension, compression, bending or torsion. In the first case many vacancies are produced (Kozinets *et al* 1977). In all cases, dislocations are the major defects that occur. An indication of the relative amounts of defects produced in deformation can be obtained by annealing experimentals. Such an experiment was performed on stretched and compressed potassium samples by Gurney and Gugan (1971). They measured the residual resistivity decrease after annealing at a series of temperatures and found that an important part of the annealing took place at a few stages with widths of 5–40 K. In figure 13, these stages are labelled A–E. The little peak around 4.5 K (stage A) is ascribed tentatively to the motion of interstitials; the broad stage B is associated with several processes involving the long-range migration of vacancies, and around 110 K (stage E) dislocations anneal out and recrystallisation may take place. According to this interpretation, both vacancies and dislocations were formed in macroscopic numbers during deformation.

Independent information on the same subject was obtained from measurements of the change in length of samples deformed at 1.2 K and annealed in subsequent stages (Gugan 1975): this experiment also showed important rearrangements going on below
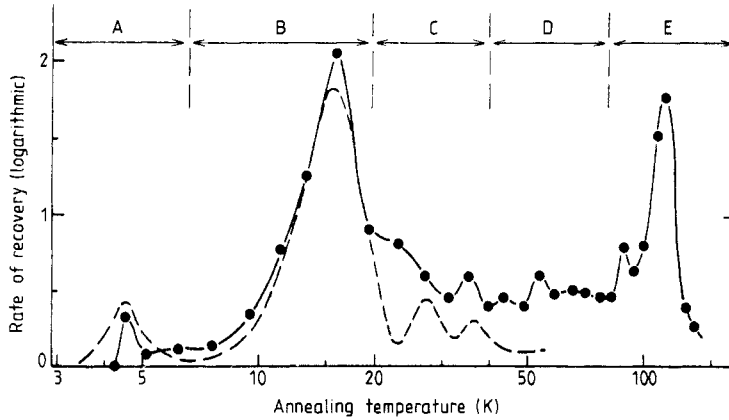
Figure 13. The annealing of deformed potassium samples (Gurney and Gugan 1971). Shown is the recovery rate (relative residual resistivity decrease) plotted against annealing temperature. The former is related to the number of defects annealing out at the given temperature. The five stages that are discerned by the authors (see text) are indicated.

20 K. Both experiments show that annealing at well-chosen temperatures can aid in controlling selectively the kind of lattice defects in the samples. In particular, in order to obtain a high dislocation density without a large number of point defects, partial annealing after deformation has been used by various groups (see, for example, van Vucht *et al* 1982).

2.7.5. Resistivity due to dislocations. In contrast to vacancies and interstitials, which may be regarded as special kinds of impurities, the nature of conduction-electron scattering by dislocations is far from clear. Both the long-range strain fields and the more sharply defined core are expected to contribute to electron–dislocation scattering, but there is not much agreement yet on which of these predominates.

The long-range strain field of a dislocation will cause primarily small-angle scattering. That such an effect is powerful is demonstrated by an elegant experiment by Zavaritskii (1975): he made a heat current flow down a torsionally strained zinc crystal. The electrons obtain a tangential momentum component from the asymmetric strain field which is present everywhere in the crystal, and thus produce a measurable magnetic field parallel to the main current direction, proportional to both current and torsion angle. In their theories concerning the interference of electron–dislocation scattering and other scattering mechanisms, Kaveh and Wiser (see the previous subsections) assume most of the scattering to be of this small-angle nature.

On the other hand, Brown (1977, 1982) considers core scattering as the most important mechanism and obtains very good agreement between experimental and calculated values for the resistivity as a function of dislocation density. He is supported by Basinski *et al* (1983) who infer from de Haas–van Alphen measurements on copper samples that, at least as far as resistivity is concerned, most of the electron–dislocation scattering must be of large-angle nature, as expected from core scattering.

The resistivity per metre of dislocation has been a subject of experimental study for many years: Basinski *et al* (1963) give a review of available data for many metals. An updated review can be found by Brown (1982). For the alkali metals, where much dislocation annealing takes place far below room temperature, experimental values of

the dislocation density are hard to give, and this entity is normally estimated from the degree of deformation and comparison with other metals. Usually ρ_d/n_d is found to be constant or just assumed so. Deviations from this 'rule' are given in Kaveh and Wiser (1983a). One important point is that Kulesko and Borzenko (1980) found that, in zinc, edge dislocations gave rise to a considerably stronger resistivity than screw dislocations; probably, this can be explained by the fact that the core of an edge dislocation is really a long row of partial vacant sites, but a screw dislocation causes far less disturbance of the background ion density.

Theoretical calculations of ρ_d/n_d have been performed by various groups; see also Basinski *et al* (1963). Among the modern calculations, Brown (1977, 1982) is very successful. He assumes the predominance of large-angle scattering by the dislocation core. Resonance states localised at the dislocation, like those proposed by Gantmakher and Kulesko (1975), play an important role in the process. A universal simple formula, which must be generally valid for the majority of metals, gives good agreement with the experimental data. Since the core is relatively small, the proximity of other dislocations is not found to influence the dislocation resistivity in this theory.

Mutual influence of dislocations was found, however, by Kaveh and Wiser (1981b, 1983a) who obtained a decreasing ρ_d/n_d as a function of n_d. Their argument is based on the same considerations as their treatment of DMR due to interference between electron–phonon, electron–electron, electron–impurity and electron–dislocation scattering (see previous subsections). Since electron–phonon scattering is involved, their curves are temperature-dependent (figure 14). Experimental evidence for these effects is not yet widely available, however. Also, Bhatia and Gupta (1970) found evidence of strong interference between various scattering sources in their calculations of ρ_d, giving a dependence of this quantity on impurity content, and causing considerable DMR.
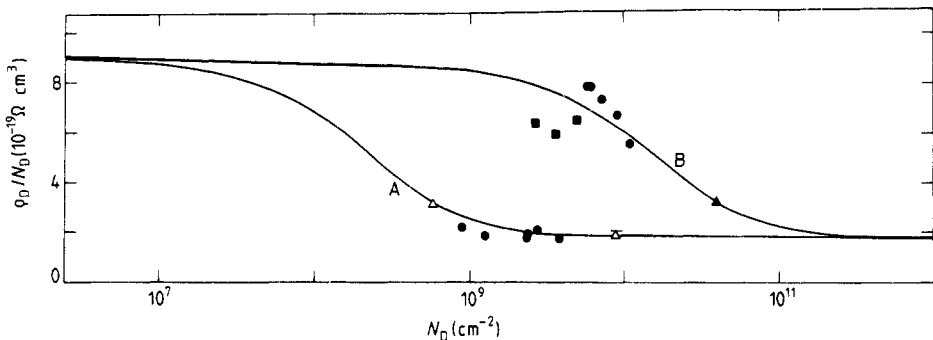

Figure 14. ρ_d/n_d as a function of n_d for aluminium at 4.2 K (A) and at 80 K (B) as predicted by Kaveh and Wiser (1983a), and some data to be compared with the theory (see Kaveh and Wiser (1983a) for references).

3. The low-temperature thermal resistivity

In contrast to the electrical resistivity, there have been no great surprises in the thermal resistivity recently. One reason for this is that the measuring precision has not made the jump of several orders of magnitude which applies to the electrical case. The other is that new effects seen in the electrical resistivity are either completely absent (phonon drag) or only visible at higher temperatures (the electron–electron term). There exists

a thermal counterpart of Matthiessen's rule and deviations from it: calculations of the latter use the same ideas as electrical resistivity calculations (and are often combined with them), giving results of the same order of magnitude for relative DMR. There exists less experimental support in the thermal case, however.

The electrical current is carried by particles with a temperature-independent charge. The thermal current, carried not only by electrons but also by phonons, is proportional to the amount of heat each of these particles bears which is proportional to T. Ignoring the phonon thermal conductivity, and assuming that the relaxation times for the thermal and electrical current are the same, a proportionality $\lambda(T) \propto \sigma(T)T$ is to be expected. Ziman (1960 §9.9) gives a general derivation of the ratio of both entities and arrives at the following result:

$$\frac{\lambda}{\sigma T} = L_0 = \frac{\pi^2 k_B^2}{3e^2}$$

where L_0 is called the (zero-temperature) Lorentz number. Apart from a slightly different value for L_0, this is the same expression as derived by Wiedemann and Franz in 1853 for a classical gas.

For this derivation to hold, it is important that the scattering mechanisms are equally effective in restoring the equilibrium electron distribution in momentum space whether the disequilibrium is produced by a temperature gradient or by an electric field. Therefore, small-angle scattering processes are excluded, since they are effective in moving electrons perpendicular to the Fermi surface: they convert 'hot' electrons into cold ones and cold electrons into hot ones. Such processes are far less important
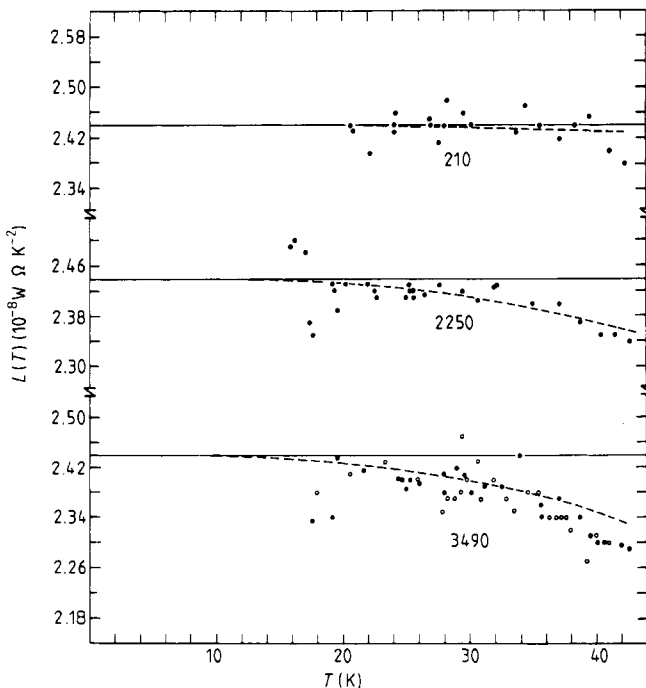

Figure 15. Lorentz ratio L as a function of T for aluminium samples with different RRR given for each curve from measurements by Amundsen *et al* (1972). Deviations from L_0 (full line) become smaller as the share of electron–impurity scattering in total scattering increases.

for the electrical resistivity. Small-angle scattering arises, for example, from electron–phonon interaction at low temperatures. At high temperatures, where high-energy phonons dominate the electron scattering, L is expected to return to L_0. At intermediate temperatures, where electron–phonon scattering is considerable but of small-angle character (or inelastic, since the electron energy varies perpendicular to the Fermi surface) the effective Lorentz number L deviates from L_0 by some tens of per cent. As an illustration, results for $L(T)$ of Al obtained by Amundsen *et al* (1972) from measurements of $\rho(T)$ and $W(T)$ on the same samples are shown in figure 15. At the low temperatures where the data were taken, the deviations from L_0 are due to the electron–phonon interaction. The lattice thermal conductivity is another, usually small, source of deviations from the Wiedemann–Franz law.

3.1. The electron–electron and electron–phonon interactions

At low temperatures the electrons are mainly scattered by impurities and phonons. The latter produce a T^2 term in the thermal resistivity at the lowest temperatures, when calculated in the Bloch limit, in contrast to a T^4 which would be expected if the Wiedemann–Franz law would be applicable to this process. Thus the total electron thermal resistivity at low T is described approximately by

$$W^e = (\lambda^e)^{-1} = \frac{\rho_0}{L_0 T} + bT^2. \tag{3.1}$$

The lattice thermal conductivity, which is added to λ, is 2–4 orders of magnitude smaller than λ for reasonably pure metals and can thus be ignored for the moment. Experimentally, this relation is obeyed in potassium from approximately 1.5 to about 10 K (figure 16, Newrock and Maxfield 1973b) with b ranging from 1.53×10^{-3} cm W^{-1} K^{-1} in pure samples to 2.38×10^{-3} cm W^{-1} K^{-1} in impure ones. A closer look at these data reveals some details which are ascribed to the onset of Umklapp
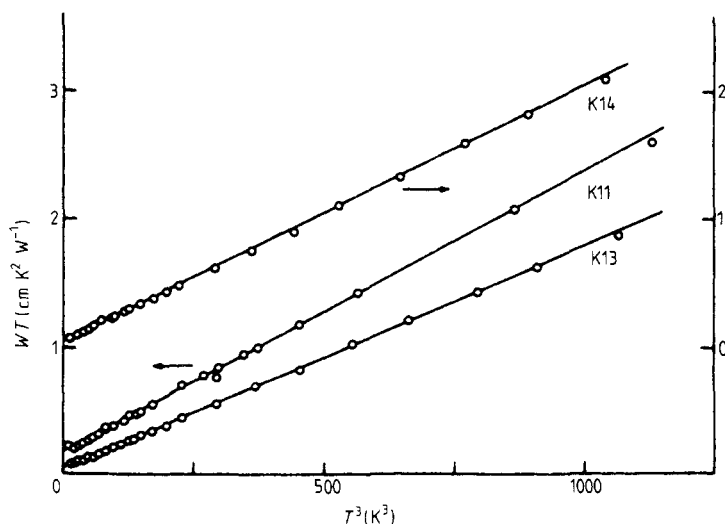

Figure 16. $W^e T$ as a function of T^3 for three potassium samples (Newrock and Maxfield 1973b): the straight lines give evidence of terms in T^{-1} (related to the residual resistivity via the Wiedemann–Franz law) and in T^2 which corresponds to electron–phonon scattering in the Bloch limit.

scattering (see calculations by Ekin (1972)). The latter is far less dominating than in the electrical conductivity because normal processes at low temperatures are of small-angle nature but Umklapp processes scatter over large angles. The picture is similar in other simple metals: for example, Rumbo (1976) measured the thermal conductivity of silver and copper samples and found the above formula to hold, apart from a somewhat lower exponent of the electron–phonon term in both metals. Also here considerable DMR were demonstrated in his pure and impure, unstrained and strained samples.

More recent calculations of W^e_{e-p} by Jumper and Lawrence (1977) and Leavens (1977) come closer to the data of Newrock and Maxfield for potassium; the latter, incorporating the energy dependence of the distribution function, is reasonably successful in explaining the 30% DMR found in the b coefficient.

The contribution from electron–electron scattering, W^e_{e-e}, is found to be proportional to T, with the coefficient of the order of $2-8 \times 10^{-4}$ cm W^{-1} in potassium, and much smaller in the polyvalent metals (calculations, for example, by Kukkonen and Smith (1973), Kukkonen and Wilkins (1979) and, with a different method, MacDonald and Geldart (1980)). This magnitude is such that the term cannot be resolved at low temperature by state-of-the-art measuring techniques, but at temperatures well above θ_D its existence can be inferred from the difference between expected and measured values of $W^e_{e-p}(T)$ and $W(T)$, respectively. Agreement between experiment and theory for K is good in this region: 2.7×10^{-4} cm W^{-1} measured by Cook (1979) as against 2.4 predicted by MacDonald and Geldart (1980).

The importance of these high-T data lies in the opportunity to compare the results to those calculated by the same methods for the low-temperature electrical resistivity. This enabled Kaveh and Wiser (1981a) to demonstrate the existence of temperature regions with different electron–electron scattering intensities because of a varying k dependence of the total relaxation time (see § 2.4).

3.2. The lattice thermal conductivity

The thermal conductivity by phonons, to be denoted as λ^g (where the g stems from the German 'Gitter' = lattice), is of interest from two points of view.

(i) It provides a method for studying the phonon–electron interaction as seen by the phonons, and the scattering of phonons by impurities, defects, etc.

(ii) Its magnitude must be known in order to draw the right conclusions from experiments on the electron thermal conductivity.

The latter point is generally unimportant in pure metals at low temperatures and in zero magnetic field, where λ^g is 10^2-10^4 times smaller than λ^e. Under the following conditions its influence becomes measurable or eventually dominant.

(a) When the sample is superconducting: then the electrons carry no heat at all, and the phonons are not scattered by electrons.

(b) In high magnetic fields: thermal magnetoresistance diminishes the electron heat current.

(c) In dilute alloys, where the impurities reduce the electron mean free path by orders of magnitude.

On the other hand, these conditions can be employed to observe λ^g. Then (a) can only be applied to a few simple metals over a very limited temperature range (Al below 1.18 K, In below 3.4 K), and since phonon–electron scattering is absent, the same λ^g is not measured as in the normal state; (b) and (c) are widely used. When using the

alloying method, alloys of different impurity concentrations (up to about 30%) are produced and their thermal resistance measured; the electronic contribution is calculated from the Wiedemann–Franz law and the ideal (electron–phonon) thermal resistivity, and subtracted from the results. Care has to be taken to be sure that the phonon–impurity scattering stays unimportant with respect to the dominant mechanism which limits λ^g. When using magnetic-field methods, an extrapolation to infinite field is supposed to eliminate the entire heat conduction by electrons but to leave λ^g unaffected. These methods are described in the next section.

At the low-temperature limit, the most important scattering mechanism which limits λ^g in most simple polyvalent metals is the phonon–electron interaction. At higher temperatures, say around $\theta_D/10$, phonon–impurity and phonon–phonon scattering start taking over (Ziman 1960 chap 8.9) so that λ^g starts at zero, attains some maximum value at about $\theta_D/10$, and falls gradually back towards zero at high temperatures.

The phonon–electron term is closely related to the electron–phonon interaction, and in the simplest approximation can be related to the ideal thermal resistivity $W_i = bT^2$ (Klemens 1969 p 61):

$$\lambda^g = \frac{313}{W_i}\left(\frac{T}{\theta_D}\right)^4 N^{-4/3}$$

where N is the number of conduction electrons per atom. This therefore yields a T^2 behaviour of λ^g at low T.

Both alloying and high-field methods have been used to determine λ^g of the polyvalent metals (for a review, see Butler and Williams (1978)), and the results for aluminium and indium show satisfying consistency among each other and with Klemens' simple formula. In figure 17, this purely quadratic behaviour is shown for aluminium. One might compare the values for Al: the formula gives $\lambda^g = 1.1 \times 10^{-4}$ W cm^{-1} K^{-1}, measurements on Al(Cu) alloys (Amundsen *et al* 1977) give 1.0 in the same units, data from Al(Mg) alloys give 0.86 (Klaffky *et al* 1975), and measurements on very pure Al samples in the high-field Corbino method which is explained below (De Lang *et al* 1978) give 1.0 for the coefficient. The T^2 form persists
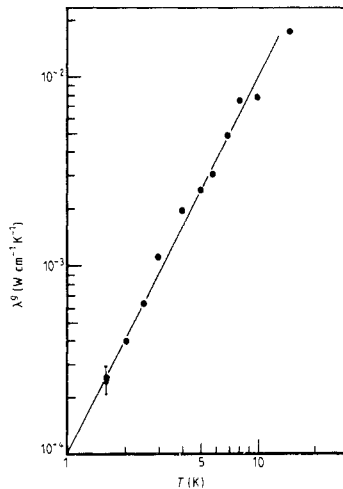

Figure 17. The lattice thermal conductivity λ^g of aluminium plotted logarithmically as a function of T. Data from De Lang *et al* (1978) measured by the Corbino method. The straight line indicates T^2 behaviour.

up to about 10 K. The Corbino method was also applied down to 0.4 K (Hubers *et al* 1972, van Kempen *et al* 1972) to indium, giving the value of $9.5 \times 10^{-4} T^2 \text{W cm}^{-1} \text{K}^{-1}$, about 1.5 times higher than the results from alloys (Sladek 1955, Butler and Williams 1978).
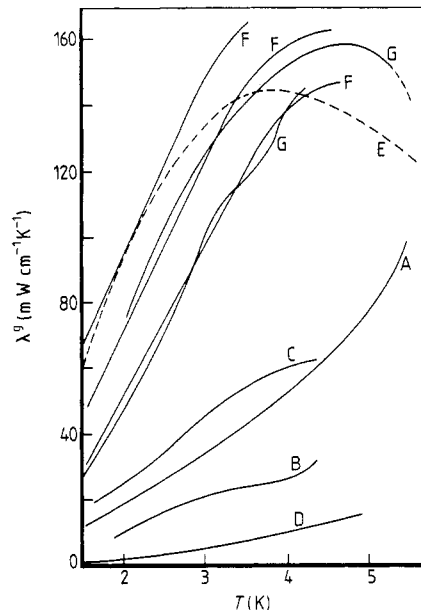

Figure 18. The lattice thermal conductivity of potassium as found by various workers. Curve A represents a calculation by Ekin (1972) assuming only phonon–electron scattering in a simple approximation. Curve B: a K(Cs) alloy (Archibald *et al* 1967); C: a K(Rb) alloy (Amundsen and Salter 1981); D: λ^g determined from high-field thermal coefficients by Tausch and Newrock (1977); E: the same data interpreted according to Fletcher's method, i.e. via the quadratic term in $W^{\text{total}}(B)$; F: high-field data from Stinson *et al* (1979a, b); G: high-field Corbino data from van Vucht *et al* (1985).

3.2.1. The alkali metals. The alkali metals present a much less simple picture. We shall concentrate on K since most of the work has been done on it. Figure 18 contains theoretical data based on a simple calculation by Ekin (1972), as well as data found by alloying with Cs (Archibald *et al* 1967), by alloying with Rb (Amundsen and Salter 1981), and by high-field methods interpreted in different ways (Stinson *et al* 1979a, b, Tausch and Newrock 1977, van Vucht *et al* 1985). There is no serious discrepancy between Ekin's calculations and the alloying results, if one takes the limited precision of both into account. The high-field results, however, are either much lower or much higher than the former. Moreover, the highest curves show a temperature dependence which is quite different from the T^2 the others find approximately. We have to take a closer look at the most used high-field methods to get some insight into possible causes of these differences.

We start by assuming that we work in the high-field limit, where $\omega_c \tau \gg 1$. For potassium of the usual purity this is true at fields $B \gg 0.05$ T, i.e. at comparatively low fields. The Lifshitz–Azbel'–Kaganov (LAK) theory (1957) predicts in this limit for the simple metals we consider that the diagonal thermal magnetoresistance saturates to a value W_0^e. However, it has been found experimentally that in the high-field limit there is always a linear term in B present. This happens both in the thermal and in the

electrical conductivity, and is treated extensively in § 4. It is found experimentally that W_0^e is practically equal to the zero-field resistivity W^e which behaves according to equation (3.1). Furthermore, there is the Righi–Leduc coefficient (the thermal counterpart of the Hall coefficient): $W_{xy}^e/B = A_{RL}$. According to LAK theory, A_{RL} should have the free-electron value $(L_0 Tne)^{-1}$, which is found to be in agreement with experiment within about 5% in the temperature region of interest (Fletcher 1977a). Thus we have for the tensor components W_{xx}^e and W_{xy}^e:

$$W_{xx}^e = W_0^e(1 + \alpha B)$$

$$W_{xy}^e = A_{RL}B$$

where W_0 is the zero-field thermal resistivity (see the previous section) and α corresponds to a thermal Kohler slope.

Inverting the tensor W^e to obtain λ^e, and adding the lattice component, we obtain

$$\lambda_{xx} = \lambda^g + \frac{W_0^e(1 + \alpha B)}{(W_0^e)^2(1 + \alpha B)^2 + (A_{RL}B)^2}$$

$$\lambda_{xy} = \frac{A_{RL}B}{(W_0^e)^2(1 + \alpha B)^2 + (A_{RL}B)^2}.$$

At the highest fields, terms W_0^e independent of B in the denominator will become negligible, and defining

$$A_1^2 = A_{RL}^2 + (W_0^e)^2\alpha^2$$

we can write

$$\lambda_{xx} = \lambda^g + \frac{W_0^e(1 + \alpha B)}{(A_1 B)^2}$$

$$\lambda_{xy} = \frac{A_{RL}}{A_1^2 B}.$$

It will be explained later that in the Corbino method λ_{xx} is measured directly. In methods other than the Corbino method, components of W are measured. We find these by inverting back from λ. The W_{xx}^{total} can be approximated at not too high fields, and if $\alpha \ll A_{RL}$ so that $A_1 = A_{RL}$, as

$$W_{xx}^{total} = W_0^e(1 + \alpha B) + \lambda^g A_{RL}^2 B^2.$$

Thus there appears to be an extra term proportional to B^2 in W_{xx} which was not expected originally, and which can be explained, in principle, completely from λ^g. Also, the Righi–Leduc coefficient A_{RL} decreases by a factor (Fletcher 1974)

$$A_{RL}^{meas} = A_{RL}^e \left(\frac{\lambda_{xx}^e}{\lambda_{xx}^e + \lambda^g} \right)^2.$$

The quadratic term in W_{xx} has indeed been observed in measurements on potassium by Newrock and Maxfield (1973a, 1976) and Tausch *et al* (1979). Fletcher (1974) attributed such a term wholly to λ^g, which rendered a very unsuspected magnitude and temperature dependence for this term. This was a reason for Tausch and Newrock (1977) to reject such an interpretation; they also measured A_{RL} and saw that this decreases much less than expected at such a large λ^g. Therefore, they adopted λ^g values which were about a factor of 15 lower and approximately quadratic in tem-

perature. They argued that another mechanism, such as open orbits from a charge density wave (see § 5), must be responsible for the B^2 term. Since in a Corbino geometry (see below) such a term arises naturally, a partial Corbino effect was proposed as an alternative by De Lang *et al* (1979). Stinson *et al* (1979a, b) remeasured W_{xx} and W_{xy} simultaneously for a small number of samples, so that they were able to determine $\lambda_{xx}^{\text{total}}$ by inverting the W tensor. They again found the large values for λ^g shown in figure 18. The situation stayed very confusing: the results of Tausch *et al* could be criticised for the quadratic term staying unexplained, and for the fact that their explanation effected too strong a field dependence of $\lambda_{xy}B$ (Fletcher and Opsal 1979); on the other hand, the small λ^g version explained why W_{xx} was not found to saturate up to 9.5 T, and removed inconsistencies regarding the thermal Kohler slopes (Tausch and Newrock 1979).

As an independent experiment, van Vucht *et al* (1985) measured λ_{xx} as a function of B and T in the Corbino configuration. In this configuration, the sample is a disc with a hole in the middle, perpendicular to the magnetic field. The heat current flows from the central hole to the outer perimeter. Contrary to the normal geometry, where the transverse heat current is forced to zero, here the transverse temperature gradient is zero because of symmetry (figure 19). Instead of W_{xx}, λ_{xx} is now found directly from the quotient of the heat current and temperature gradient. This offers two advantages: first, only the infinite field limit of one quantity has to be deduced from the data instead of two elements of a matrix to be inverted. Second, if $\alpha \ll A_{\text{RL}}$, the electronic contribution to λ_{xx} in the Corbino configuration decreases mainly with B^{-2} in contrast to $(W_{xx}^e)^{-1}$ in the conventional geometry which decreases only with B^{-1}.

The Corbino results are easy to interpret and make a clear extrapolation to infinite field possible. The corresponding curves are also to be found in figure 18: they confirm the 'high' results of Stinson *et al* and the rejected interpretation of Tausch and Newrock's data. Furthermore, the electronic part of λ_{xx}, which must be equal to $W_0^e A_{\text{RL}}^{-2} B^{-2}$ if $\alpha \simeq 0$ (which was in reasonable agreement with the data) gives the established zero-field behaviour of W_0 (see the previous subsection) if for A_{RL} the free-electron value is taken. These results suggest that the lattice conductivity of K really behaves like the upper curves in figure 18.
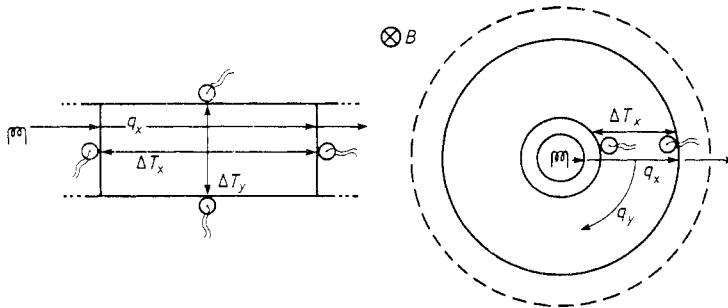

Figure 19. Rectangular and Corbino geometry compared. The magnetic field is perpendicular to the sample plane. In the usual rectangular geometry, the heat current flows from the left to the right but cannot have a transverse component: one can measure ΔT_x and ΔT_y which render W_{xx}^{total} and W_{xy}^{total}. In the Corbino geometry, the heat current flows radially from the centre hole to the outer perimeter and will have a tangential component, which is formed by electrons spiralling logarithmically towards the perimeter. Here, ΔT is radial because of symmetry: $\lambda_{xx}^{\text{total}}$ is measured directly.

Since λ^g of K does not show the T^2 dependence found in polyvalent metals, at least not between 2.5–7 K, another mechanism must be responsible. A clue can be found in a calculation by Albers *et al* (1976) who found that for most phonons electron–phonon scattering is dominant below about 10 K, but there is a class of low momentum transverse phonons which are far less sensitive to scattering by electrons than the majority of phonons. This is the same phonon group which might be responsible for phonon drag quenching in the presence of dislocations (Engquist 1982; see § 2.2). Between 2.5–4 K, the main scatterer for this group of phonons might indeed be dislocations. The sample dependence of the absolute magnitude of the data in that temperature range support this. The sample dependence of λ^g of Al(Mg) alloys has been found by Klaffky *et al* (1975) to go like T^2 upon deformation. Calculations on this base have been performed by Madarasz and Szmulowicz (1983) for Cu(Al) alloys, and by Stinson *et al* (1979a) for their potassium samples. The results of the latter authors are confirmed by their measurements of the Nernst–Ettinghausen coefficient ϵ_{xy}. Both calculations suffer from the need of very high dislocation densities ($>10^{10}$–10^{11} cm^{-2}) for a substantial effect, which is excessive in view of the dislocation densities found generally in undeformed samples (see Gugan 1982 and § 2).

Around 4 K, phonon–impurity scattering may start governing λ^g. This can explain the discrepancy between the dilute alloy results (Amundsen and Salter 1981, Archibald *et al* 1967) and the high-field data for potassium. However, the effect of impurities is not always very clear: in Al(Ag) alloys they may even increase λ^g (Amundsen and Verbeek 1976).

4. Linear magnetoresistance

4.1. Introduction

When a magnetic field is applied to a sample carrying a current, its resistance will increase because, most simply put, the electrons, deflected from their straight path by the Lorentz force, have to travel longer distances. The most quoted semiclassical calculation, which was carried out by Lifshitz *et al* (1957) (LAK theory), predicts that this increase will saturate in the high-field limit ($\omega_c \tau \gg 1$, i.e. for most pure metals saturation must be reached below 1 T). The situation is different for compensated metals (i.e. metals with equal numbers of holes and electrons) which show a B^2 dependence. The LAK theory also predicts a more involved behaviour if the Fermi surface is multiply connected in such a way that the electrons can move along open orbits in momentum space. The noble metals, which do show open orbits, are hence no longer considered simple in this section. They show a magnetoresistivity $\propto B^2$ up to the highest fields along certain directions. Nevertheless, in polycrystalline samples open orbit directions are wildly distributed with the result that on the average a linear magnetoresistance is measured (see, for example, Martin *et al* 1977).

Whatever method, sample shape, purity or dislocation density was used, experiments have always shown a linearly increasing magnetoresistance (LMR) in the high-field limit (see figure 20) in simple and other metals. Only in some cases, notably in aluminium at $B > 5$ T, do deviations occur which are thought to arise from magnetic breakdown, a tunnelling phenomenon due to deformation of the Fermi surface by the magnetic field which enables electrons to follow open orbits (see, for example, Delaney 1974).
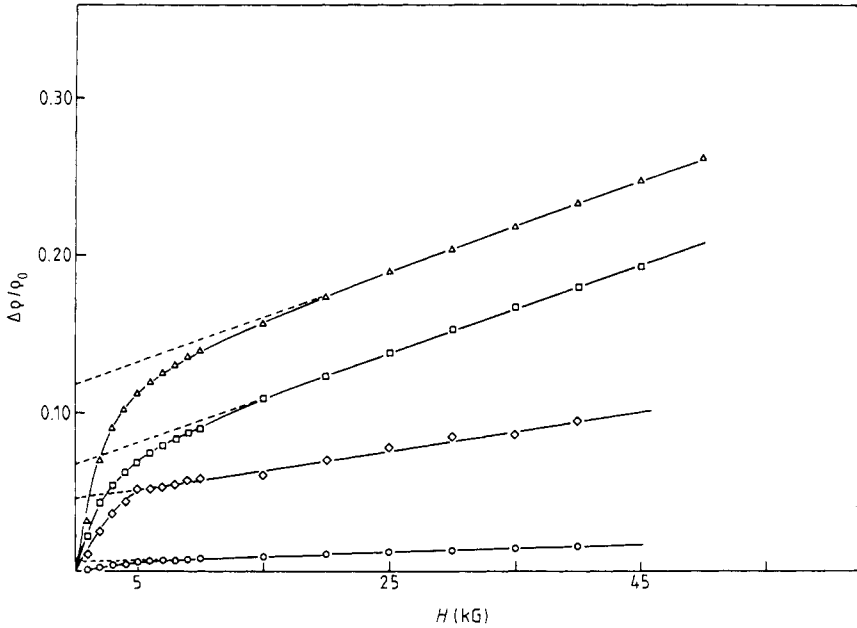
Figure 20. Resistivity as a function of field at 4.2 K for four potassium samples (Taub *et al* 1971). At low fields, the resistivity increases with B^2 according to LAK theory, which predicts saturation at high fields where $\omega_c\tau = (eB/mc)\tau \gg 1$. The linear behaviour in this region is typical up to the highest fields. The slope of this part, normalised to the Hall constant, is called the Kohler slope S and has been studied for many years as a function of several parameters. $\triangle$, KX10, $\frac{1}{2}$ h anneal, RRR = 970, $\square$; KX18, 1 h anneal, RRR = 2535; $\diamondsuit$, KX6, 4 h anneal, RRR = 720; $\bigcirc$, KX21, $\frac{1}{2}$ h anneal, RRR = 390.

Experimental procedures used are mostly four-terminal DC resistance measurements and the induced torque method (see, for example, Douglas and Datars 1974), but there exist others, e.g. various methods based on helicons (Delaney 1974). The latter author studied the magnetoresistance of an aluminium sphere by three different inductive methods and found LMR in each case. One has to conclude therefore that LMR is not an artefact of an experimental arrangement, but a very general phenomenon. Only in compensated metals, the field dependence has been found to be B^2 (experiments on Cd, W and Pb: Fletcher (1977a, b)).

A common measure of the field dependence in the high-B limit is the dimensionless Kohler slope:

$$S = \frac{\Delta\rho}{\rho\Delta(\omega_c\tau)} = \frac{\Delta\rho}{R_H\Delta B}$$

where R_H is the Hall constant and Δ are the mean differences between high-field values. In general, S varies widely with the experimental method, temperature, sample orientation (if it is a single crystal), purity, dislocation density, shape and surface roughness. General trends are: S is much larger for transverse than for longitudinal magnetoresistance; it increases with temperature and dislocation density, but often decreases with impurity content. S is mostly of the order of 10^{-3}–10^{-1}.

Also in the thermal resistivity, the high-field behaviour is linear, but here the linearity region also has an upper limit caused by the lattice thermal conductivity (see

§ 3 and references there). There is no direct correspondence between the electrical and thermal Kohler slopes.

4.2. Explanations of linear magnetoresistance

An impressive number of theories have been proposed to explain data which are still not understood. A few of these will be mentioned here. They can be divided into intrinsic and extrinsic theories, i.e. theories which depend only on the bulk properties of the material and those which depend on sample-dependent factors.

Among the intrinsic theories are those that consider magnetic breakdown as the underlying mechanism. In a magnetic field a redistribution of the electrons on the Fermi surface due to the extra constraint that their orbits must satisfy Landau quantisation takes place. This reshapes the Fermi surface into a set of coaxial rings which coincide with the zero-field Fermi surface approximately, but not completely. Therefore, at high fields open orbits may exist which are not present at zero field. When Fermi surface sheets in adjacent Brillouin zones are close to each other but not touching, tunnelling may become possible which provides an opportunity for part of the electrons to follow open orbits. This provides a smooth transition from the no-open-orbit regime to the open-orbit regime.

Open orbits caused by a deformation of the Fermi surface of the alkali metals by a charge density wave ground state have been proposed by Reitz and Overhauser (1968) to explain linear magnetoresistance in potassium.

Also intrinsic is a theory based on anisotropic static fluctuations in the electron gas ground state due to electron–electron or electron–phonon interactions (Falicov and Smith 1972). Intrinsic theories are discredited, however, by the important dependence of S on external factors mentioned above.

Of the extrinsic causes, field inhomogeneity is usually easily discarded by well-controlled experimental conditions. The question of dislocations is more difficult: Jones (1969) measured the LMR of Na and K samples and found that S decreased upon stretching them; on the other hand, Penz and Bowers (1968), measuring the LMR of K by a helicon technique, saw S increasing upon straining the samples. G J C L Bruls (unpublished) found no significant difference in LMR between samples with many crystallite boundaries (which can be regarded as dislocation arrays) and the same samples after recrystallisation to a few large grains by annealing. Van Gelder (1978a, b) was able to show that electron scattering from bound states at a dislocation would produce LMR. Yet, this calculation is hard to test quantitatively if the effect ever proves important.

The effect of impurities on the magnetoresistance is studied by various workers (e.g. Mertig and Mrosan 1982, Mahan 1983). The latter shows that the different asymmetry of electron–phonon and electron–impurity scattering in a field can cause LMR. The size of S will be strongly dependent on the share of the phonons in the total scattering. Quantitative results are still lacking. More absolute predictions are made by theories considering macroscopic voids or inclusions (Herring (1960), Stroud and Pan (1976), Sampsell and Garland (1976) and Esposito *et al* (1979) for the thermal case). These have been tested successfully, also quantitatively, by Beers *et al* (1978a, b). These authors measured the LMR of indium wires with varying numbers of voids or glass rods embedded in the samples. The Kohler slopes were approximately proportional to the number of voids or rods, and were much smaller for longitudinal than for transverse fields, as usual. Poorly conducting inclusions should have a similar

effect. Such a theory cannot be generalised to the limit of small inhomogeneities (e.g. point defects or impurities) to give any observable effect (Landauer 1978).

The sample shape has been predicted to have an important influence on the high-field magnetoresistivity for the induced torque experiment by Lass (1970). It was obvious to also apply this theory to the four-point geometry. Two facts support such an approach: first, the Kohler slope has been observed to vary considerably in samples of the same material and purity at the same temperature. Second, Hall voltages are very geometry-dependent; the importance of Hall voltages for magnetoresistivity has been well-known for a long time, e.g. by the fact that in compensated metals, where no Hall voltages occur, the magnetoresistivity is found to show a different field dependence. Furthermore, Bruls *et al* (1981) find that for samples like those in figure 21, the magnetoresistance of each segment is remarkably different and that, in the case of the wedge, the data taken on one side of the sample differ enormously from those taken on two opposite contacts (figure 22). The relation between Hall voltages and linear magnetoresistance is therefore an obvious field to explore. This has been done by the same authors (Bruls *et al* 1981, 1984) by writing down the high-field transport equation (Lifshitz *et al* 1957):

$$E = \rho(J + \beta \times J)$$

where $\beta = (R_H/\rho)B$. Under the condition $\nabla \cdot J = 0$, one can solve this equation by averaging over the sample's direction parallel to the field and making a transformation of the other components into the complex plane. The solutions show in a straightforward way that if the sample cross section is not constant, the Hall voltages on both sides of the sample behave differently, and that the voltage difference between two probes is, in the high-field limit, linear in the field. The solutions demonstrate that large current distortions in the direction perpendicular to current and field take place. The experiments by Bruls *et al* are in complete quantitative agreement with exact solutions so obtained for a rectangular groove, a rectangular projection and a wedge-shaped part of the sample.

The Bruls–van Gelder model gives much larger effects than would be obtained if the above-mentioned void theories were generalised to 'half-voids' on the surface. A P van Gelder (unpublished) has shown that this model and void theory are mutually inconsistent for finite width samples; the generalisation fails since the void models
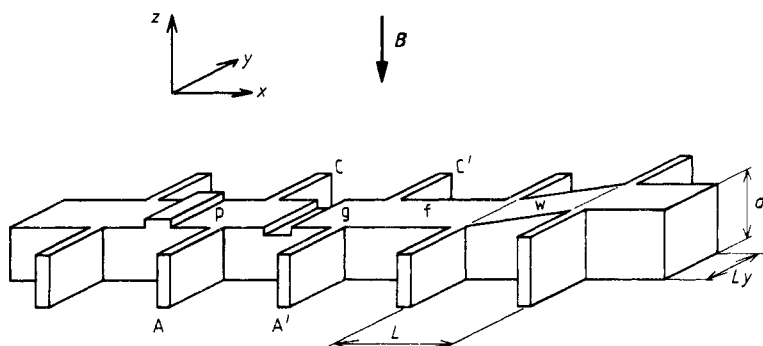

Figure 21. Aluminium sample used by Bruls *et al* (1981) showing potential contacts on both sides of the sample between regions where different kinds of variations in the sample dimension parallel to the field are machined. There is one flat region for reference.
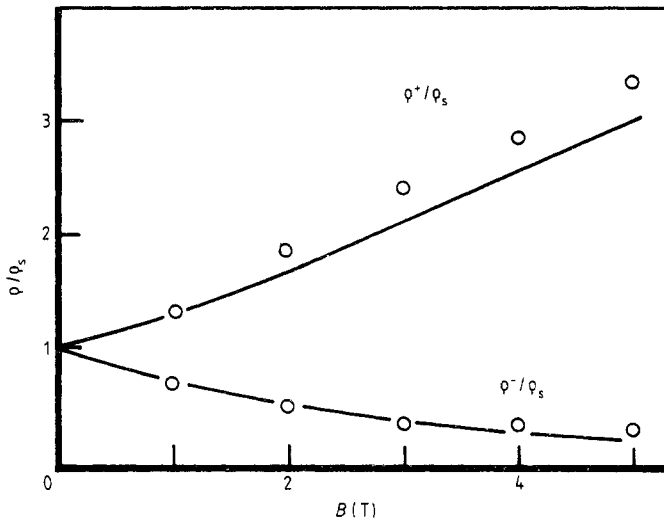
Figure 22. Resistivity as a function of field as measured on two opposite pairs of contacts comprising the wedge-shaped region of the sample shown in figure 21. The full curves are calculated according to the Bruls–van Gelder model. According to their interpretation the large differences between voltages on opposite contact pairs are due to differences in Hall voltage.

imply averaging along the length of the voids, rather than over the field direction. Measurements on samples like those in figure 21 with different widths have shown Kohler slopes increasing with the width, in agreement with the Bruls–van Gelder model. An intriguing implication of the model is that the number of cross-section changes is far more important for the Kohler slope than the length between changes: three grooves of width 0.1 mm and distance 0.1 mm have a larger effect than one groove of equal depth and a width of 0.3 mm. This explains why surface roughness has been observed to be an important parameter. A separate measurement of the thermal magnetoconductivity of a sample like that in figure 21 has also been performed and has shown that the same model applies here.

Summarising, it is found that only models dealing with macroscopic geometrical aspects of the samples have been successful so far in explaining quantitatively much of the observed LMR. The additivity of these models is still a topic of discussion, but likely to hold in samples with not too exotic geometrical parameters. In view of these results, much of the old LMR data should be re-examined critically.

5. Charge density waves in the alkali metals

Much work has been spent both theoretically and experimentally during the past decade on investigating the possible occurrence in the alkali metals of charge density waves (CDW). A metal sample containing a CDW is expected to show fundamental differences with respect to 'normal' metals, in which the electron density is uniform. From the time CDW were proposed by Overhauser (1968), this alternative theory was often claimed to give a better description of the unexplained outcome of several experiments than the simple nearly-free-electron models that are usually applied to the alkali metals. In many cases, refinements of the 'classical' theories have afterwards

been able to account for these previously unexplained data, but still there are a few experiments for which this has not happened, and the results of which cannot be ascribed to experimental difficulties. Therefore, we briefly describe the basic ideas and the impact CDW should have on various properties, and we mention a number of performed and proposed experiments which were or are claimed to be indicative of CDW.

The CDW theory postulates a lower symmetry than the body-centred cubic structure of the alkali metals. A lower symmetry causes extra Brillouin zone boundaries to show up in momentum space. These (nearly) cut the Fermi surface and thus make it deviate essentially from a spherical one which is characteristic for the alkali metals.

According to CDW theory (see Overhauser (1978) for a review), the electron density in an alkali metal is modulated unidirectionally:

$$\rho(r) = \rho_0[1 + p \cos(Q \cdot r + \varphi)]$$

where p is a modulation depth (of the order of tens of per cent), Q is the characteristic vector of the CDW and φ is an arbitrary phase term. The lattice then deforms sinusoidally in order to maintain overall charge neutrality. The new periodicity imposed by Q has a wavelength $2\pi/Q$ of the order of three times the lattice constant but incommensurable to it. This causes two new Bragg planes to arise in the first Brillouin zone, almost touching the Fermi surface. The regions of the Fermi surface closest to these planes then protrude to touch them because of the interaction with the lattice (cf the rounding of the Fermi surface at Bragg planes in polyvalent metals). At the same time, a gap shows up in the band structure about the Fermi level which causes the energy for electrons close to the new Bragg planes to decrease. The total energy of the electron system was shown by Overhauser to be lower in this situation than in the absence of a CDW because of exchange and correlation effects. The existence of open orbits parallel to Q is caused by the connection to the adjacent Brillouin zone provided by the new necks. There exist 48 preferred directions for Q, about 4° away from [110] directions (Giuliani and Overhauser 1979).

An important implication of the lattice deformation is the occurrence of excitations of such a structure in which the phase φ varies sinusoidally in time and space. These excitations are called phasons and can be described by the superposition of two coherent phonons, but behave differently as far as their dispersion relation is concerned. They are thought to be an independent source of electron scattering, of specific heat terms, etc.

A general sample will not possess one global Q vector, but will be divided, according to theory, into many domains with different Q, even if the sample is a single crystal. Several of the CDW properties that will be mentioned are insensitive to this disorder, but the detection of open-orbit effects requires that the domains be much larger than the electron mean free path. Any experiment concerned with the latter that fails to give clear evidence of these open orbits must be suspected of having too small domains. One way out follows from an argument by Boriack (1980) who calculates the magnetic-field susceptibility of a CDW and concludes that cooling samples in a large magnetic field (several T) will eventually direct all Q, thus providing a method to obtain single Q-domain samples.

In a few experiments, small oil drops on the sample surface have been observed to change the sample properties. It has been suggested often that the strain which the sample undergoes because of differences in contraction at cooling down causes an alignment of the Q vectors.

CDW have been invoked to explain several experimental observations.

(*a*) An unexpected gap in the optical absorption of K (El Naby 1963). Later on, however, it was proved that only a K sample covered with a thin KOH layer would produce such a gap (Overhauser and Butler 1976, Taut 1982).

(*b*) A Hall constant in potassium decreasing at high fields to a few per cent below the free-electron value (Penz 1968) which was attributed to open orbits arising from a CDW state. More recent measurements have given values closer to the free-electron value: for a review of these, see Fletcher (1977a).

(*c*) A linear magnetoresistance in alkali and simple polyvalent metals (§ 4) which has been tentatively ascribed to magnetic breakdown. As such a process is only possible in metals where the Fermi surface comes close to the Brillouin zone boundaries one has to invoke a CDW structure (Reitz and Overhauser 1968) to provide the necessary distortion of the Fermi surface.

(*d*) A term proportional to $T^{1.5}$ in the electrical resistivity (Rowlands *et al* 1978) which was tentatively ascribed to electron–phason scattering (Bishop and Overhauser 1979, 1981). It was shown in § 2.4 that there is no reason any more to consider this term as a real bulk property of potassium.

(*e*) A small peak in the specific heat of alkali metals around about 1 K which compares well with the calculated specific heat of phasons. Measurements (Lien and Phillips 1964, Martin 1970, Amarasekara and Keesom 1981, 1982a) and calculations (Giuliani and Overhauser 1980, Taylor *et al* 1981, Phillips 1982, MacDonald and Taylor 1982, Amarasekara and Keesom 1982b) centred on the question of the existence of the small peaks. Since the experimental uncertainties are almost as large as the postulated peaks in all experiments, the situation remains rather obscure.

(*f*) Deviations from Matthiessen's rule. The CDW situation was shown by Sharma (1980) to lead to deviations from Matthiessen's rule. Clearly, this prediction will have to be tested rigorously by theoretical refinement and experiment in order to survive comparison with the other DMR sources mentioned in § 2.3.

(*g*) A four-fold anisotropy in induced torque measurements on spherical single-crystal potassium samples (Schaefer and Marcus 1971, Elliott and Datars 1983). The four-fold anisotropy was explained by Overhauser (1971a) by means of CDW, but also by Lass (1972, 1976) by assuming that the samples deviated from ideal sphericity.

New induced torque measurements at higher fields (Coulter and Datars 1980, 1982) show, above 5 T, a much richer structure than the relatively smooth four-fold-anisotropic curves at lower fields (see figure 23). Between 1.1 and 1.9 K, many of the peaks show a temperature dependence. The obvious identification of these peaks with open-orbit directions (Overhauser 1982) is somewhat hampered by the difficulty of predicting the exact directions of this wealth of sharp maxima, as well as of the T dependence. The general structure is well accounted for, however (Huberman and Overhauser 1981).

Several experiments have been or could obviously be proposed for giving more conclusive evidence of a CDW structure.

(*h*) Deviations from sphericity of the Fermi surface are easily studied by the de Haas–van Alphen (DHVA) effect. Up till now no evidence for CDW has been found (Templeton 1981, O'Shea and Springford 1981). It can be argued, however, that because of the CDW the Fermi surface has, like the polyvalent metals, strongly curved regions near the Bragg planes where electron–phonon scattering is much more intense than on the spherical part of the surface. This reduces the chance of observing electrons passing through the vicinity of such a neck by DHVA signals. Assuming that the samples consist of a large number of Q domains, the majority of the signal picked up in a
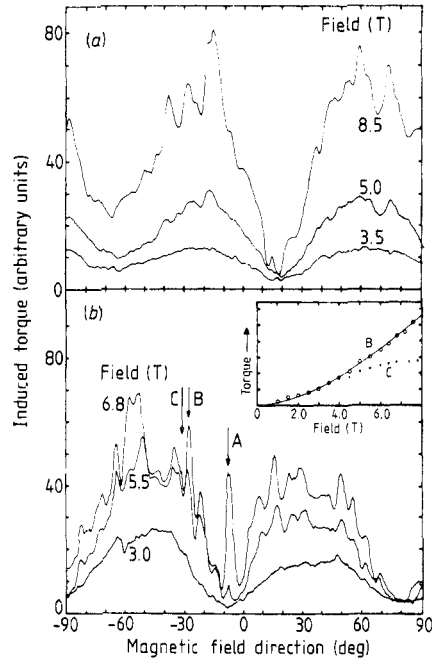
Figure 23. Angular dependence of the induced torque of potassium at a number of field strengths (Coulter and Datars 1980). The four-fold anisotropy dominating at the lower fields is a common feature, but the spikes at high fields have only been observed in potassium and are strongly temperature-dependent. They are tentatively ascribed to open orbits. (*a*) Sample grown in oil, (*b*) sample grown in a mold. The insert shows that the field dependence in a peak is close (not equal) to B^2, and different between peaks.

specific direction will be determined by the electrons in domains where this direction corresponds to a circular orbit. Therefore, DHVA experiments can only be conclusive when one can argue that the samples must definitely be single-domain samples.

(*i*) A CDW structure would produce a special type of $1/f$ noise, called 'magnetoflicker noise' (Overhauser 1974). Hockett and Lazarus (1974) sought for this between 10 Hz and 10 kHz but could not detect such a noise, even though their sensitivity was sufficient to detect a contribution with a factor of 1000 less intensity than predicted.

(*j*) The periodic lattice deformation which accompanies a CDW should be observable in neutron diffraction experiments, via satellite peaks (Overhauser 1971b). Werner *et al* (1980) did the experiment but saw nothing, whereupon Giuliani and Overhauser (1981) argued that a higher sensitivity is needed to observe the effect.

(*k*) In a single-domain crystal, the residual resistivity should show a large anisotropy. The amplitude of this was first calculated by Bishop and Overhauser (1977, 1978) as about 4 to 1. Later calculations (De Gennaro and Borchi 1982a, b) reduced the effect to a factor of about 1.5, which is difficult to observe on one sample in subsequent runs in view of the usual irreproducibility of the RRR. Only by an experiment where the residual resistivity is measured at the same time parallel to and perpendicular to the expected Q (perhaps directed by cooling in a large field), one has a chance of finding this anisotropy.

This long list of ups and downs for the CDW theory shows why a general acceptance of the theory is still far out of sight, and even becoming less probable. Yet, arguments against it are not yet completely compelling as long as most samples can be thought

of as having many small Q domains, if any, and the anomalous high-field induced torque data still have found no other explanation. The critical experiment has still to be done. We can think of the following suggestions.

(i) Before any experiment, the sample must preferably be cooled in a strong magnetic field (at least 5 T).

(ii) Experiments between 1–2 K, and may be in fields above 5 T, have the largest chance of being successful, according to the region where Coulter and Datars claim to see open orbits.

(iii) X-ray transmission experiments under these circumstances are extremely difficult, but because of the clear indication they can give of a periodic lattice distortion, they should be considered.

(iv) Microwave transmission experiments on K similar to those performed by Lubzens *et al* (1977) on copper, which showed the existence of open orbits in that metal.

(v) Magnetoresistance experiments on single crystals which can be rotated in a strong magnetic field should show a smooth small magnetoresistance as a function of orientation (§ 4), but if open orbits exist, superposed on this will be sharp peaks where the magnetoresistance becomes quadratic as a function of the field. Such experiments are being undertaken at present. Also thermal magnetoresistance experiments should show such an effect (Huberman and Overhauser 1982), but this kind of measurement is probably much more difficult.

(vi) Also, theorists are challenged to find alternative explanations of the high-field torque data.

6. Conclusions

The foregoing sections have shown that a number of phenomena which were unknown some two decades ago have become established facts in DC transport in simple metals. The importance of phonon drag in the phonon-limited electrical resistivity in the alkali metals has been established. Electron–electron scattering, both in the low-temperature electrical resistivity and in the high-temperature thermal resistivity, is now fully accepted. The problem of the conflicting results concerning the lattice thermal conductivity of potassium has been clarified. An outstanding accomplishment of the last 10 years is that theoretical predictions have got quantitatively very close to the experimentally found resistivity contributions for the temperature-dependent scattering processes. However, it seems more difficult to predict the residual resistivity components precisely. In particular, the precise mechanism of electron–dislocation scattering is still not well understood.

The role of interference between different scattering processes has been demonstrated exhaustively in the research on deviations from Matthiessen's rule. Both ρ_{e-e} and ρ_{e-p} are clearly affected by factors that were thought to be felt only in the residual resistivity. Most of the interference is caused by differences in relaxation time anisotropy in momentum space. Only phonons at high temperatures are completely isotropic. Even impurities show a certain variation over the Fermi surface, which can be large in the alkali metals. Also, the extra effectiveness of small-angle scattering of electrons near the Brillouin zone boundaries in decreasing the conductivity has been proved to be important. Quantitative predictions of the effect of impurities and lattice imperfections on the temperature-dependent resistivity are now in agreement with experiment, typically to within a factor of 2. The crucial question remaining is whether

the increase of the electron–electron interaction in the alkali metals is really due to dislocations. If the apparent increase is caused by some other mechanism which exerts its influence mainly below 0.5 K, conclusions on DMR in ρ_{e-e} must be revised thoroughly. Therefore, highly sensitive experiments in this temperature region on simple metals under a variety of conditions are urgently needed.

The electron thermal conductivity profited from the same progress in basic understanding as the electrical conductivity, apparently leaving no great problems. Although the lattice thermal conductivity of the polyvalent metals is well-understood, in potassium something exotic seems to be going on: either a special class of phonons has a completely different sensitivity to the usual scattering mechanisms, or something completely novel is happening. Independent experiments on phonon transport, e.g. ultrasound attenuation, are needed to verify the current ideas.

Among the high-field properties, the linear magnetoresistance posed the largest theoretical problem during the last decades. We believe that the major importance of geometry (external and internal: voids and badly conducting inclusions) has been established. For these aspects quantitative agreement between theory and experiment has been attained. The four-fold anisotropy seen in the induced torque experiments appears to be explainable from geometrical sources, too. Only the spike structure of induced torque data on potassium remains an exotic feature, which is at present the last stronghold of the charge density wave model. An independent experiment which provides broader evidence for this model is needed to prevent it falling into oblivion.

Our main conclusion is that the most interesting things are now going on far below 1 K, and maybe above 5 T: the regions where simple metals become much less simple.

Acknowledgments

References

Abrikosov A A 1972 *Introduction to the theory of normal metals* (New York: Academic)
Adlhart W, Stetter G, Fritsch G and Luscher E 1981 *J. Phys. F: Met. Phys.* **11** 1347-60
Albers R C, Bohlin L, Roy M and Wilkins J W 1976 *Phys. Rev.* B **13** 768-86
Aleksandrov B N 1971 *Fiz. Met. Metall.* **31** 1175-85
Aleksandrov B N, Kan Ya S and Tatishvili D G 1974 *Fiz. Met. Metall.* **37** 1150-8
Amarasekara C D and Keesom P H 1981 *Phys. Rev. Lett.* **47** 1311-3
—— 1982a *Phys. Rev.* B **26** 2720-6
—— 1982b *Phys. Rev. Lett.* **48** 1506
Amundsen T, Furuseth O and Søvik R P 1977 *J. Phys. F: Met. Phys.* **7** L159-63
Amundsen T, Myhre A and Salter J A M 1972 *Phil. Mag.* **25** 513-7
Amundsen T and Salter J A M 1981 *Phys. Rev.* B **23** 931-4
Amundsen T and Verbeek B H 1976 *Physica* **81BC** 319-22
Archibald M A, Dunick J E and Jericho M H 1967 *Phys. Rev.* **153** 786-95
Ashcroft N W 1963 *Phil. Mag.* **8** 2055-83
Ashcroft N W and Mermin N D 1976 *Solid State Physics* (New York: Holt, Rinehart and Winston)
Awasthi O N 1981 *Physica* **107B** 135-6

Awasthi O N and Sathish S 1981 *Phys. Lett.* **83A** 283-6
Babić E, Krsnik R and Očko M 1976 *J. Phys. F: Met. Phys.* **6** 73-83
Babushkina N A, Zhernov A P and Inyushkin A V 1982 *Sov. Phys.-JETP* **55** 469-73
Bailyn M 1958 *Phys. Rev.* **112** 1587-98
—— 1960 *Phys. Rev.* **120** 381-404
Barber A J and Caplin A D 1975 *J. Phys. F: Met. Phys.* **5** 679-96
Barnard B R, Caplin A D and Dalimin M N B 1981 *Phil. Mag. B* **44** 711-29
—— 1982 *J. Phys. F: Met. Phys.* **12** 719-44
Basinski Z S, Coleridge P T, Howie A, Lonzarich G G and Sigfusson T I 1983 *J. Phys. F: Met. Phys.* **13** L233-8
Basinski Z S, Dugdale J S and Howie A 1963 *Phil. Mag.* **8** 1989-97
Bass J 1972 *Adv. Phys.* **21** 431-604
—— 1982 *Landholt-Börnstein Tables* New Series III/15a (Berlin: Springer-Verlag)
Beers C J, van Dongen J C M, van Kempen H and Wyder P 1978a *J. Physique* **39** C6 1126-7
—— 1978b *Phys. Rev. Lett.* **40** 1194-7
Bergmann A, Kaveh M and Wiser N 1974 *Phys. Rev. Lett.* **32** 606-9
—— 1980a *J. Phys. F: Met. Phys.* **10** L71-6
—— 1980b *Solid St. Comm.* **34** 369-73
—— 1981 *Phys. Rev. B* **24** 6807-19
—— 1982a *J. Phys. F: Met. Phys.* **12** 2985-3008
—— 1982b *J. Phys. F: Met. Phys.* **12** 3009-30
Bhatia A B and Gupta O P 1970 *Phys. Rev. B* **1** 4577-84
Bishop M F and Overhauser A W 1977 *Phys. Rev. Lett.* **39** 632-5
—— 1978 *Phys. Rev. B* **18** 2447-63
—— 1979 *Phys. Rev. Lett.* **42** 1776-9
—— 1981 *Phys. Rev. B* **23** 3638-54
Black J E 1972 *Can. J. Phys.* **50** 2355-8
—— 1978 *Can. J. Phys.* **56** 708-14
—— 1980 *Phys. Rev. B* **21** 3279-86
Bobel G, Cimberle M R, Napoli F and Rizzuto C 1976 *J. Low Temp. Phys.* **23** 103-17
Borchi E and De Gennaro S 1980 *J. Phys. F: Met. Phys.* **10** L271-4
Boriack M L 1980 *Phys. Rev. Lett.* **44** 208-10
Brody M, Kaveh M and Wiser N 1981 *Physica* **108B/C** 1165-6
Brown R A 1977 *J. Phys. F: Met. Phys.* **7** 1283-95
—— 1982 *Can. J. Phys.* **60** 766-78
Bruls G J C L, Bass J, van Gelder A P, van Kempen H and Wyder P 1981 *Phys. Rev. Lett.* **46** 533-5
—— 1985 *Phys. Rev. B* to be published
Butler W H and Williams R K 1978 *Phys. Rev. B* **18** 6483-94
Caplin A D and Rizzuto C 1970 *J. Phys. C: Solid St. Phys.* **3** L117-20
Cimberle M R, Bobel G and Rizzuto C 1974 *Adv. Phys.* **23** 639-71
Cook J G 1979 *Can. J. Phys.* **57** 1216-23
Coulter P G and Datars W R 1980 *Phys. Rev. Lett.* **45** 1021-4
—— 1982 *Solid St. Comm.* **43** 715-8
Cowley R A, Woods, A D B and Dolling G 1966 *Phys. Rev.* **150** 487-94
Dagens L and Perrot F 1973 *Phys. Rev. B* **8** 1281-92
Dagens L, Rasolt M and Taylor R 1975 *Phys. Rev. B* **11** 2726-34
Danino M, Kaveh M and Wiser N 1981a *J. Phys. F: Met. Phys.* **11** L107-11
—— 1981b *J. Phys. F: Met. Phys.* **11** 2563-73
—— 1982 *J. Phys. F: Met. Phys.* **12** L259-65
—— 1983 *J. Phys. F: Met. Phys.* **13** 1665-76
Daybell M D 1967 *Rev. Sci. Instrum.* **38** 1412-5
De Gennaro S and Borchi E 1982a *J. Phys. F: Met. Phys.* **12** 963-8
—— 1982b *J. Phys. F: Met. Phys.* **12** 2363-76
De Lang H N, van Kempen H and Wyder P 1978 *J. Phys. F: Met. Phys.* **8** L39-42
—— 1979 *Phys. Rev. B* **20** 809-11
Delaney J A 1974 *J. Phys. F: Met. Phys.* **4** 247-55
Dosdale T and Morgan G J 1974 *J. Phys. F: Met. Phys.* **4** 402-18
Douglas R J and Datars W R 1974 *Solid St. Comm.* **14** 461-4
Dugdale J S and Basinski Z S 1967 *Phys. Rev.* **157** 552-63
Dynes R C and Carbotte J P 1968 *Phys. Rev.* **175** 913-9

Edmunds D L, Pratt W P Jr and Rowlands J A 1980 *Rev. Sci. Instrum.* **51** 1516-22
Ekin J W 1971 *Phys. Rev. Lett.* **26** 1550-3
—— 1972 *Phys. Rev.* B **6** 371-6
Ekin J W and Bringer A 1973 *Phys. Rev.* B **7** 4468-78
Ekin J W and Maxfield B W 1971 *Phys. Rev.* B **4** 4215-25
Elliott M and Datars W R 1983 *J. Phys. F: Met. Phys.* **13** 1483-500
El Naby M H 1963 *Z. Phys.* **174** 269-79
Endo T and Kino T 1979 *J. Phys. Soc. Japan* **46** 1515-21
Engquist H L 1982 *Phys. Rev.* B **25** 2175-84
Esposito F P, Newrock R S and Loeffler K 1979 *Phys. Rev.* B **20** 2348-61
Falicov L M and Smith H 1972 *Phys. Rev. Lett.* **29** 124-7
Fickett F R 1971a *Cryogenics* **11** 349-67
—— 1971b *Phys. Rev.* B **3** 1941-52
Fletcher R 1974 *J. Phys. F: Met. Phys.* **4** 1155-61
—— 1977a *Phys. Rev.* B **15** 3602-8
—— 1977b *Solid St. Commun.* **21** 1139-42
Fletcher R and Opsal J L 1979 *Phys. Rev.* B **20** 2555
Fleurov V N, Kondratenko P S and Kozlov A N 1980 *J. Phys. F: Met. Phys.* **10** 1953-73
Fröböse K 1977 *Z. Phys.* B **26** 19-27
Gantmakher V F and Kulesko G I 1975 *Sov. Phys.-JETP* **40** 1158-60
Garland J C and Bowers R 1969 *Phys. Kondens. Mater.* **9** 36-44
Giuliani G F and Overhauser A W 1979 *Phys. Rev.* B **20** 1328-31
—— 1980 *Phys. Rev. Lett.* **45** 1335-8
—— 1981 *Phys. Rev.* B **23** 3737-43
Gugan D 1971 *Proc. R. Soc.* A **325** 223-49
—— 1975 *Phil. Mag.* **31** 453-63
—— 1982 *J. Phys. F: Met. Phys.* **12** L173-8
Gurney W S C and Gugan D 1971 *Phil. Mag.* **24** 857-78
Gurzhi R N 1963 *Sov. Phys.-JETP* **17** 521-2
Gurzhi R N and Kopeliovich A I 1981 *Sov. Phys.-Usp.* **24** 17-41
Haerle M L, Pratt W P Jr and Schroeder P A 1983 *J. Phys. F: Met. Phys.* **13** L243-8
Hayman B and Carbotte J P 1971 *Can. J. Phys.* **49** 1952-66
—— 1973 *Can. J. Phys.* **51** 1109-19
Herring C 1960 *J. Appl. Phys.* **31** 1939-53
Hockett R S and Lazarus D 1974 *Phys. Rev.* B **10** 4100-11
Huberman M and Overhauser A W 1981 *Phys. Rev. Lett.* **47** 682-5
—— 1982 *Phys. Rev.* B **25** 7071-4
Hubers M, Klein J F M, van Kempen H, De Lang H N, Lass J S, Miedema A R and Wyder P 1972 *Proc.
     Int. Conf. on Phonon Scattering in Solids* ed H J Albany (Saclay: Service de Documentation du CEN)
     p 169
Jansen A G M, van Gelder A P and Wyder P 1980 *J. Phys. C: Solid St. Phys.* **13** 6073-118
Jones B K 1969 *Phys. Rev.* **179** 637-8
Jumper W D and Lawrence W E 1977 *Phys. Rev.* B **16** 3314-21
Kagan Yu and Zhernov A P 1966 *Sov. Phys.-JETP* **23** 737-47
—— 1971 *Sov. Phys.-JETP* **33** 990-6
Kaveh M 1977 *Phys. Rev.* B **15** 3788-95
Kaveh M, Leavens C R and Wiser N 1979 *J. Phys. F: Met. Phys.* **9** 71-8
Kaveh M and Wiser N 1972a *Phys. Rev.* B **6** 3648-58
—— 1972b *Phys. Rev. Lett.* **29** 1374-7
—— 1974a *Phys. Rev.* B **9** 4042-52
—— 1974b *Phys. Rev.* B **9** 4053-9
—— 1974c *Phys. Lett.* **49A** 47-8
—— 1975 *Phys. Lett.* **51A** 89-90
—— 1977 *Solid St. Commun.* **23** 927-30
—— 1979 *Solid St. Commun.* **29** 531-5
—— 1980a *J. Phys. F: Met. Phys.* **10** L37-42
—— 1980b *Phys. Rev.* B **21** 2278-90
—— 1980c *Phys. Rev.* B **21** 2291-308
—— 1981a *J. Phys. F: Met. Phys.* **11** 419-28

—— 1981b *J. Phys. F: Met. Phys.* **11** 1749-63
—— 1982 *J. Phys. F: Met. Phys.* **12** 935-50
—— 1983a *J. Phys. F: Met. Phys.* **13** 953-61
—— 1983b *J. Phys. F: Met. Phys.* **13** 1207-11
Khoshnevisan M, Pratt W P Jr, Schroeder P A and Steenwyk S D 1979a *Phys. Rev.* B **19** 3873-8
Khoshnevisan M, Pratt W P Jr, Schroeder P A, Steenwyk S and Uher C 1979b *J. Phys. F: Met. Phys.* **9** L1-5
Klaffky R W, Mohan N S and Damon D H 1975 *Phys. Rev.* B **11** 1297-307
Klemens P G 1969 *Thermal Conductivity* vol 1 (New York: Academic)
Koshino S 1960 *Prog. Theor. Phys.* **24** 1049-54
—— 1963 *Prog. Theor. Phys.* **30** 415-20
Kozinets V V, Khotkevich V I and Filips A Kh 1977 *Sov. J. Low Temp. Phys.* **3** 734-7
Krill G 1971 *Solid St. Commun.* **9** 1065-8
Kukkonen C A and Smith H 1973 *Phys. Rev.* B **8** 4601-6
Kukkonen C A and Wilkins J W 1979 *Phys. Rev.* B **19** 6075-93
Kulesko G I and Borzenko T B 1980 *Sov. Phys.-Solid St.* **22** 443-7
Landau L and Pomeranchuk I 1936 *Phys. Z. Sowj.* **10** 649
Landauer R 1978 *J. Phys. F: Met. Phys.* **8** L245-50
Lass J S 1970 *J. Phys. C: Solid St. Phys.* **3** 1926-33
—— 1972 *Phys. Lett.* **39A** 343-4
—— 1976 *Phys. Rev.* B **13** 2247-53
Lawrence W E 1975 *Phys. Rev.* B **12** 4161-83
—— 1976 *Phys. Rev.* B **13** 5316-9
Lawrence W E and Wilkins J W 1972 *Phys. Rev.* B **6** 4466-82
—— 1973 *Phys. Rev.* B **7** 2317-32
Leavens C R 1977 *J. Phys. F: Met. Phys.* **7** 1297-304
Leavens C R and Laubitz M J 1974 *Solid St. Commun.* **15** 1909-13
—— 1975 *J. Phys. F: Met. Phys.* **5** 1519-32
Lee C W, Haerle M L, Heinen V, Bass J, Pratt W P Jr, Rowlands J A and Schroeder P A 1982 *Phys. Rev.* B **25** 1411-4
Lee C W, Pratt W P Jr, Rowlands J A and Schroeder P A 1980 *Phys. Rev. Lett.* **45** 1708-11
Lee M J G 1969 *Phys. Rev.* **178** 953-65
—— 1971 *CRC Crit. Rev. Solid St. Sci.* **2** 85-120
Levy B, Sinvani M and Greenfield A J 1979 *Phys. Rev. Lett.* **43** 1822-5
Lien W H and Phillips N E 1964 *Phys. Rev.* **133** A1370-7
Lifshitz I M, Azbel' M Ia and Kaganov M I 1957 *Sov. Phys.-JETP* **4** 41-54
Llewellyn B, Paul D McK, Randles D L and Springford M 1977a *J. Phys. F: Met. Phys.* **7** 2531-44
—— 1977b *J. Phys. F: Met. Phys.* **7** 2545-54
Lubzens D, Grunzweig-Genossar J and Schultz S 1977 *Phys. Rev.* B **16** 2474-8
MacDonald A H 1980 *Phys. Rev. Lett.* **44** 489-93
MacDonald A H and Geldart D J W 1980 *J. Phys. F: Met. Phys.* **10** 677-92
MacDonald A H and Taylor R 1982 *Phys. Rev. Lett.* **48** 1505
MacDonald A H, Taylor R and Geldart D J W 1981 *Phys. Rev.* B **23** 2718-30
Madarasz F L and Szmulowicz F 1983 *Phys. Rev.* B **28** 1763-71
Mahan G D 1983 *J. Phys. F: Met. Phys.* **13** L257-63
Martin D L 1970 *Can. J. Phys.* **48** 1327-39
Martin P M, Sampsell J B and Garland J C 1977 *Phys. Rev.* B **15** 5598-611
Matthiessen A and Vogt C 1864 *Ann. Phys., Lpz.* **122** 19
Mertig I and Mrosan E 1982 *J. Phys. F: Met. Phys.* **12** 3031-8
Meyer J, Dolling G, Kalus J, Vettier C and Paureau J 1976 *J. Phys. F: Met. Phys.* **6** 1899-914
Mitchel W, Newrock R S and Wagner D K 1980 *Phys. Rev. Lett.* **44** 426-9
Newrock R S and Maxfield B W 1973a *Solid St. Commun.* **13** 927-30
—— 1973b *Phys. Rev.* B **7** 1283-95
—— 1976 *J. Low Temp. Phys.* **23** 119-42
O'Keefe P M and Goddard W A III 1969 *Phys. Rev. Lett.* **23** 300-3
Orlov V G 1975 *Sov. Phys.-Solid St.* **16** 2175-9
O'Shea M J and Springford M 1981 *Phys. Rev. Lett.* **46** 1303-6
Overhauser A W 1968 *Phys. Rev.* **167** 691-8
—— 1971a *Phys. Rev. Lett.* **27** 938-41
—— 1971b *Phys. Rev.* B **3** 3173-82

—— 1974 *Phys. Rev.* B **9** 2441-7
—— 1978 *Adv. Phys.* **27** 343-63
—— 1982 *Can. J. Phys.* **60** 687-92
Overhauser A W and Butler N R 1976 *Phys. Rev.* B **14** 3371-6
Penz P A 1968 *Phys. Rev. Lett.* **20** 725-6
Penz P A and Bowers R 1968 *Phys. Rev.* **172** 991-1001
Perdew J P and Vosko S H 1974 *J. Phys. F: Met. Phys.* **4** 380-93
Phillips N E 1982 *Phys. Rev. Lett.* **48** 1504
Pinchuk I I 1976 *Sov. Phys.-Solid St.* **18** 64-6
Reitz J R and Overhauser A W 1968 *Phys. Rev.* **171** 749-53
Ribot J H J M, Bass J, van Kempen H and Wyder P 1979 *J. Phys. F: Met. Phys.* **9** L117-22
Ribot J H J M, Bass J, van Kempen H, van Vucht R J M and Wyder P 1981 *Phys. Rev.* B **23** 532-51
Rowlands J A, Duvvury C and Woods S B 1978 *Phys. Rev. Lett.* **40** 1201-4
Rowlands J A and Woods S B 1978 *J. Phys. F: Met. Phys.* **8** 1929-39
Roy M 1974 *Pramana* **2** 273-81
Rumbo E R 1976 *J. Phys. F: Met. Phys.* **6** 85-98
Sambles J R and Preist T W 1982 *J. Phys. F: Met. Phys.* **12** 1971-87
Sampsell J B and Garland J C 1976 *Phys. Rev.* B **13** 583-9
Schaefer J A and Marcus J A 1971 *Phys. Rev. Lett.* **27** 935-8
Schroeder P A, Blumenstock B, Heinen V, Pratt W P Jr and Steenwyk S 1981 *Physica* **107B** 137-8
Senoussi S and Campbell I A 1973 *J. Phys. F: Met. Phys.* **3** L19-21
Sharma S M 1980 *J. Phys. F: Met. Phys.* **10** L47-9
Shukla R C and Taylor R 1976 *J. Phys. F: Met. Phys.* **6** 531-44
Sinvani M, Greenfield A J, Bergmann A, Kaveh M and Wiser N 1981a *J. Phys. F: Met. Phys.* **11** 149-63
Sinvani M, Greenfield A J, Danino M, Kaveh M and Wiser N 1981b *J. Phys. F: Met. Phys.* **11** L73-8
Sladek R J 1955 *Phys. Rev.* **97** 902-15
Srivastava P L and Singh R M 1976 *J. Phys. F: Met. Phys.* **6** 1819-26
Steenwyk S D, Rowlands J A and Schroeder P A 1981 *J. Phys. F: Met. Phys.* **11** 1623-33
Stinson M R, Fletcher R and Leavens C R 1979a *J. Phys. F: Met. Phys.* **9** L107-11
—— 1979b *Phys. Rev.* B **20** 3970-90
Stroud D and Pan F P 1976 *Phys. Rev.* B **13** 1434-8
Taub H, Schmidt R L, Maxfield B W and Bowers R 1971 *Phys. Rev.* B **4** 1134-52
Tausch P J and Newrock R S 1977 *Phys. Rev.* B **16** 5381-9
—— 1979 *Phys. Rev.* B **20** 2556-7
Tausch P J, Newrock R S and Mitchel W 1979 *Phys. Rev.* B **20** 501-14
Taut M 1982 *J. Phys. F: Met. Phys.* **12** 2019-34
Taylor P L 1964 *Phys. Rev.* **135** A1333-5
Taylor R 1978 *Solid St. Commun.* **28** 167-70
—— 1982 *Can. J. Phys.* **60** 725-34
Taylor R and Glyde H R 1976 *J. Phys. F: Met. Phys.* **6** 1915-22
Taylor R, Leavens C R, Duesbery M S and Laubitz M J 1978 *J. Physique* **39** C6 1058-9
Taylor R, Leavens C R and Shukla R C 1976 *Solid St. Commun.* **19** 809-11
Taylor R and MacDonald A H 1980 *J. Phys. F: Met. Phys.* **10** 2387-94
Taylor R, MacDonald A H and Shukla R C 1981 *Phys. Rev. Lett.* **46** 434-6
Templeton I M 1981 *J. Low Temp. Phys.* **43** 293-325
Trofimenkoff P N and Ekin J W 1971 *Phys. Rev.* B **4** 2392-7
Tsoi V S, Baas J, Benistant P A M, van Kempen H, Paijens E L M and Wyder P 1979 *J. Phys. F: Met. Phys.*
    9 L221-6
van der Mass J, Huguenin R and Rizzuto C 1981 *Physica* **107B** 139-40
van der Maas J, Rizzuto C and Huguenin R 1983 *J. Phys. F: Met. Phys.* **13** L53-8
van Gelder A P 1978a *J. Physique* **39** C6 1124-5
—— 1978b *Solid St. Commun.* **28** 481-3
van Kempen H, De Lang H N, Lass J S and Wyder P 1972 *Phys. Lett.* **42A** 277-8
van Kempen H, Lass J S, Ribot J H J M and Wyder P 1976 *Phys. Rev. Lett.* **37** 1574-7
van Kempen H, Neijenhuijsen H W and Ribot J H J M 1979 *Rev. Sci. Instrum.* **50** 161-4
van Kempen H, Ribot J H J M and Wyder P 1978 *J. Physique* **39** C6 1048-9
—— 1981 *J. Phys. F: Met. Phys.* **11** 597-614
van Vucht R J M, Schroeder P A, van Kempen H and Wyder P 1985 to be published
van Vucht R J M, van de Walle G F A, van Kempen H and Wyder P 1982 *J. Phys. F: Met. Phys.* **12** L217-21

Werner S A, Eckert J and Shirane G 1980 *Phys. Rev.* B **21** 581-4

Wyder P 1965 *Phys. Kondens. Mater.* **3** 263-91

Yamashita J 1982 *J. Phys. F: Met. Phys.* **12** 713-8

Yu Z Z, Haerle M, Zwart J W, Bass J, Pratt W P Jr and Schroeder P A 1983 *Phys. Lett.* **97A** 61-4

—— 1984 *Phys. Rev. Lett.* **52** 378-71

Zavaritskii N V 1975 *Sov. Phys.-JETP* **40** 601-4

Ziman J M 1960 *Electrons and Phonons* (Oxford: Clarendon)

—— 1972 *Principles of the theory of solids* (Cambridge: Cambridge University Press)

Zwart J W, Pratt W P Jr, Schroeder P A and Caplin A D 1983 *J. Phys. F: Met. Phys.* **13** 2595-602